

Accepted Manuscript

Synthesis, *in silico* experiments and biological evaluation of 1,3,4-trisubstituted pyrazole derivatives as antimalarial agents

Adnan A. Bekhit, Manal N. Saudi, Ahmed M.M. Hassan, Salwa M. Fahmy, Tamer M. Ibrahim, Doaa Ghareeb, Aya M. El-Seidy, Sherry N. Nasralla, Alaa El-Din A. Bekhit



PII: S0223-5234(18)31026-2

DOI: <https://doi.org/10.1016/j.ejmech.2018.11.067>

Reference: EJMECH 10925

To appear in: *European Journal of Medicinal Chemistry*

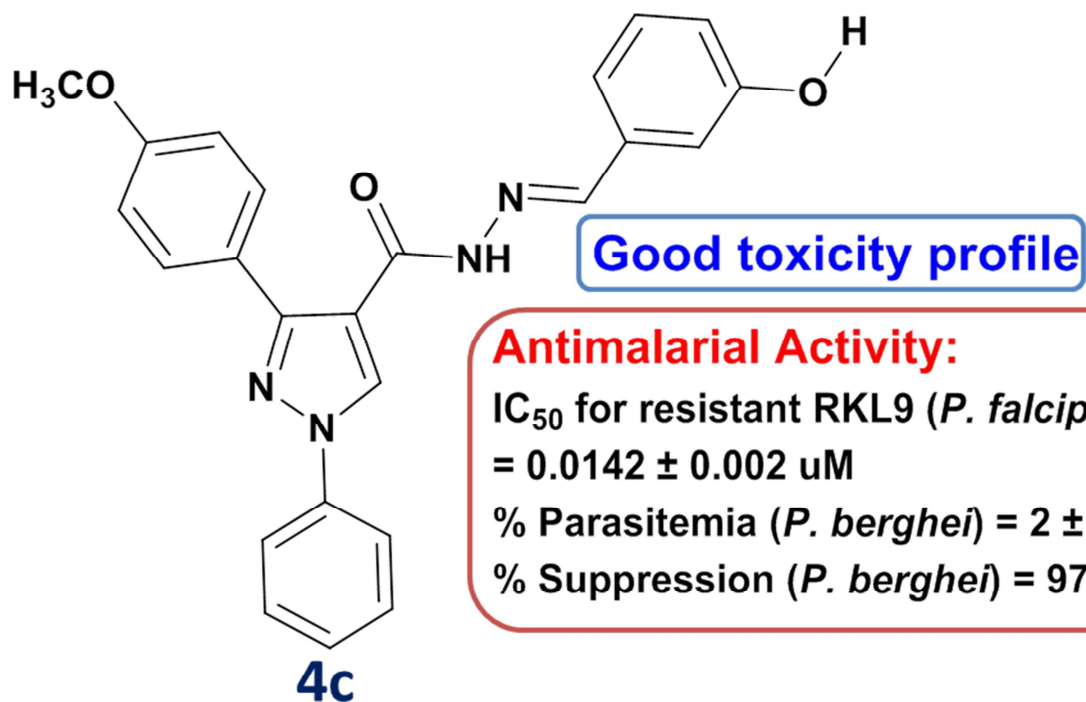
Received Date: 24 September 2018

Revised Date: 5 November 2018

Accepted Date: 28 November 2018

Please cite this article as: A.A. Bekhit, M.N. Saudi, A.M.M. Hassan, S.M. Fahmy, T.M. Ibrahim, D. Ghareeb, A.M. El-Seidy, S.N. Nasralla, A.E.-D.A. Bekhit, Synthesis, *in silico* experiments and biological evaluation of 1,3,4-trisubstituted pyrazole derivatives as antimalarial agents, *European Journal of Medicinal Chemistry* (2019), doi: <https://doi.org/10.1016/j.ejmech.2018.11.067>.

This is a PDF file of an unedited manuscript that has been accepted for publication. As a service to our customers we are providing this early version of the manuscript. The manuscript will undergo copyediting, typesetting, and review of the resulting proof before it is published in its final form. Please note that during the production process errors may be discovered which could affect the content, and all legal disclaimers that apply to the journal pertain.



ACCEPTED MANUSCRIPT

Synthesis, *in silico* experiments and biological evaluation of 1,3,4-trisubstituted pyrazole derivatives as antimalarial agents

Adnan A. Bekhit^{a,b*}, Manal N. Saudi^a, Ahmed M. M. Hassan^a, Salwa M. Fahmy^a, Tamer M. Ibrahim^{c,d}, Doaa Ghareeb^e, Aya M. El-Seidy^a, Sherry N. Nasralla^b, Alaa El-Din A. Bekhit^f

^aDepartment of Pharmaceutical Chemistry, Faculty of Pharmacy, Alexandria University, Alexandria 21521, Egypt

^bPharmacy Program, Pharmacology Stream, Allied Health Department, College of Health Sciences, University of Bahrain, P.O. Box 32038, Kingdom of Bahrain

^cPharmaceutical Chemistry Department, Faculty of Pharmacy, Kafrelsheikh University, Kafr El-Sheikh 33516, Egypt.

^dPharmaceutical Chemistry Department, Faculty of Pharmacy, The British University in Egypt, Al-Sherouk City, Cairo, Egypt

^eDepartment of Biochemistry, Faculty of Science, Alexandria University, Alexandria, Egypt

^fFood Sciences, University of Otago, Dunedin, New Zealand

Correspondence: Adnan A. Bekhit,
Department of Pharmaceutical Chemistry,
Faculty of Pharmacy, Alexandria University, Alexandria
21521, Egypt.

E-mail: adnbekhit@pharmacy.alexu.edu.eg

Fax: 20-3-4873273

1 Abstract

New 1,3,4-trisubstituted pyrazole derivatives were synthesized and evaluated for their antiplasmodial activity. Compounds **4b**, **4c**, **7a** and **7d** were the most potent antiplasmodial agents against *P. berghei* with percent of suppression ranging from 90-100 %. They were also screened for their *in vitro* antimalarial activity against the chloroquine resistant strain *P. falciparum*, (RKL9). Compound **4c** displayed the highest *in vitro* antimalarial activity; 13-fold higher than standard chloroquine phosphate. Molecular docking of the most active compounds against the wildtype and quadruple mutant *pf* DHFR-TS structures rationalized the *in vitro* antimalarial activity. Furthermore, these compounds exhibited reasonable *in silico* drug-likeness and pharmacokinetic properties. Toxicity studies of the most active compounds revealed that all tested compounds were non-toxic and well-tolerated up to 150 mg/kg via oral route and 75 mg/kg via parenteral route. According to RBC hemolysis assay, it was found that compound **7a** was the most potent anti-inflammatory and least toxic derivative with IC₅₀ value 71-fold higher than IC₅₀ value related to the antimalarial activity. Moreover, cytotoxicity assessment revealed that compound **4c** was the least toxic derivative with IC₅₀ value 70000-fold higher than IC₅₀ value related to the antimalarial activity.

Key words

Pyrazole, hydrazone, oxadiazole, triazole, thiazole, thiazolidinone, thiadiazole, antimalarial, *in silico* experiments, cytotoxicity, RBCs hemolysis and acute toxicity.

2 Introduction

Malaria is one of the most significant parasitic diseases endemic to Africa and parts of Asia. It is caused by four species of *Plasmodium* genus, but only two species are responsible for the majority of infections; *P. falciparum* and *P. vivax* [1]. According to the WHO report in 2016, although there is a substantial decline in the number of malaria cases and malaria deaths, the disease accounted for 420,000 deaths in the year 2015, mainly in African children under five years old. [2]. In addition, more than 50% of population is exposed to malaria risk in Ethiopia. The main cause of infection is *Plasmodium vivax*, followed by *P. falciparum* and mixed infection [3]. Despite the many interventions planned and adopted by malaria-inflicted countries, further strategies should be implemented to target 90% or more reduction in the global malaria incidence and mortality. One of the most important obstacles to complete malaria eradication, is the rapidly developing resistance and severe adverse effects of currently used drugs [2, 3]. In order to decrease the incidence of developing resistance, combinations of two or more drugs is recommended. These drugs should target multiple stages of parasitic life cycles as sporozoites, hypnozoites, merozoites and gametocytes. They also should include transmission blocking compounds and ensure post-treatment prophylaxis [4-6]. Therefore, there is a crucial need to synthesize new derivatives, with a wider safety margin, capable of targeting novel pathways and enzymes inside protozoa. Also, there is a need to develop new innovative strategies to ensure sustainable treatment and eradication of parasitic diseases. These strategies include generating new formulations with variable combinations and strengths of existing drugs, drug repurposing or repositioning and piggy-back approaches [7, 8].

Antifolates, such as pyrimethamine and cycloguanil are inhibitors of DHFR domain of *Plasmodium falciparum* dihydrofolate reductase thymidylate synthase (*pf* DHFR-TS). This inhibition leads to prevention of DNA synthesis, growth, proliferation and finally parasitic cell death [9-11]. It is worth mentioning that the resistance to pyrimethamine and its analogues appeared quickly due to site specific amino acid mutation that led to a steric clash between the previous compounds and Asn 108 [12, 13]. There is an ongoing need to discover new antimalarial agents which are effective against the mutant *pf* DHFR.

It is well known that pyrazole ring, whether free or hybridized with other heterocyclic rings, displayed a wide array of biological activities, such as antibacterial, antiviral, antitubercular, anti-inflammatory, antioxidant, anticancer, antimalarial and antileishmanial [14-23]. For instance, hybridization strategies of pyrazole ring with different scaffolds such as thiazolidinone **A** showed promising *in vivo* and *in vitro* antimalarial activities especially for the chloroquine-resistant strain of *P. falciparum* (RKL9) [24]. Also, other hybridization approaches with heterylhydrazone **B** [25], oxadiazole **C**, [26, 27] were observed to enhance antiprotozoal activity [24]. Also, heterocyclic moieties containing thiazole **D**, thiadiazole **E**, and triazole **F** [28, 29] comprised a range of promising antiprotozoal agents, as seen in **Figure**

1. Based on such rational and promising results of previously reported analogues of (A), a series of Schiff bases **I** were designed and obtained via condensation of acid hydrazide derivatives with different heterocyclic aldehydes. Also, new hybrids of pyrazoles with 4-thiazolidinones **II**, 3,4-diarylthiazoles **III**, thia- / oxadiazoles **IV** and triazoles **V** were also designed, then synthesized and biologically evaluated (**Figure 2**) as an effort to extend the chemical space of pyrazole-based chemotypes [30] for antimalarial activity.

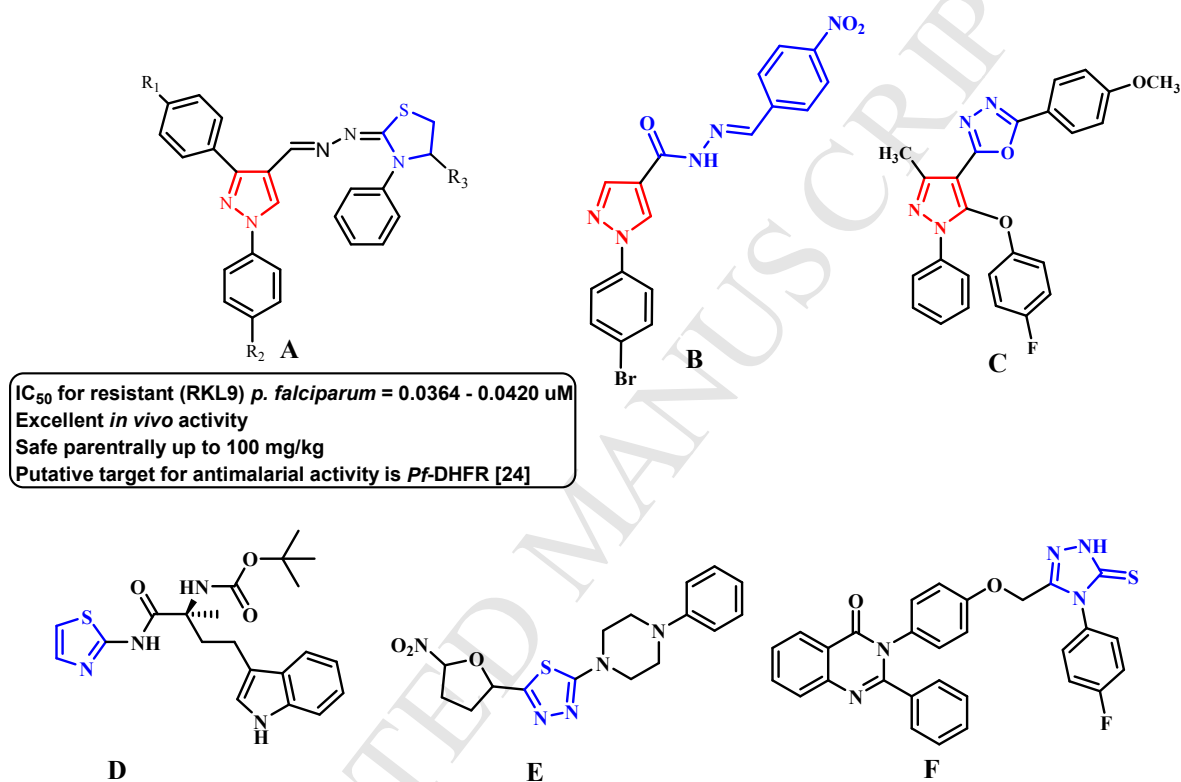


Figure 1. Rational and structures of lead antimalarial compounds.

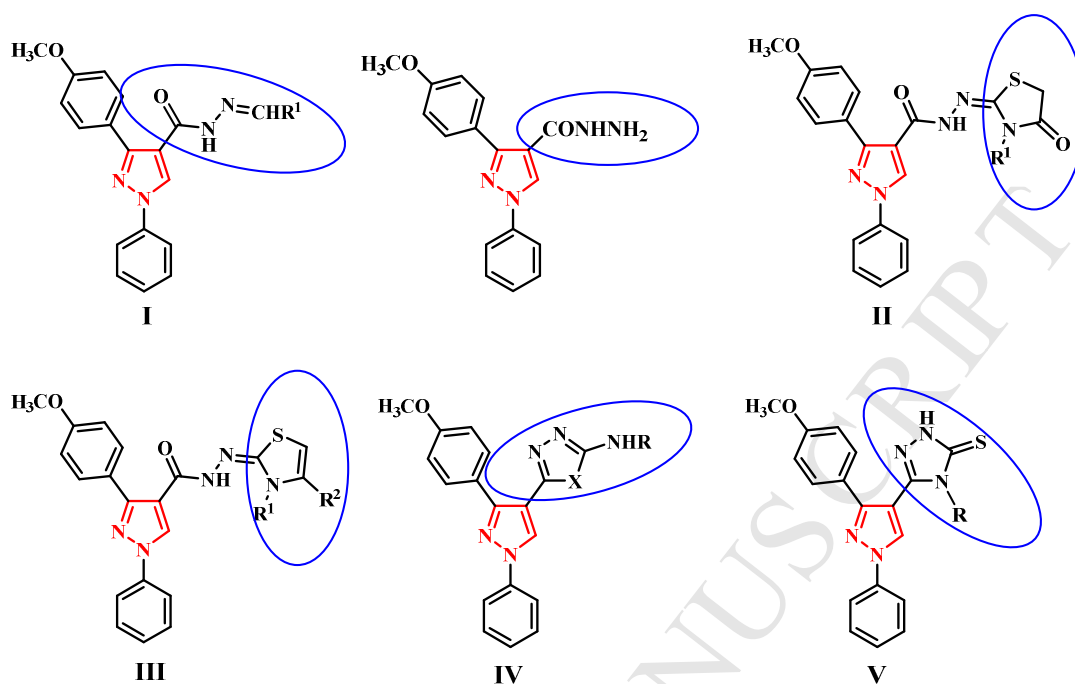


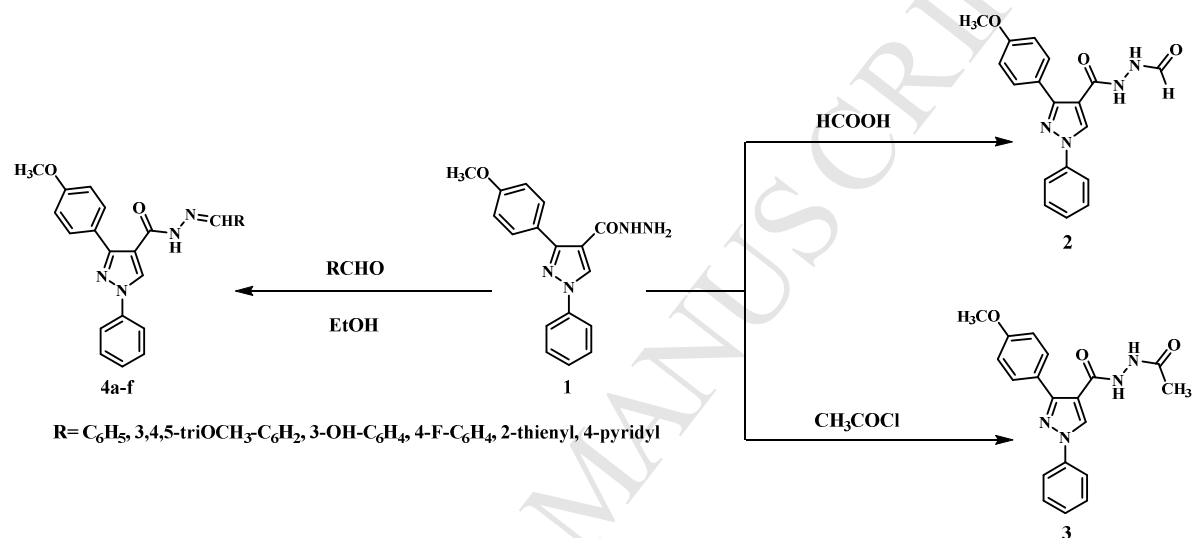
Figure 2. General formulae of the target compounds.

3 Results and discussion

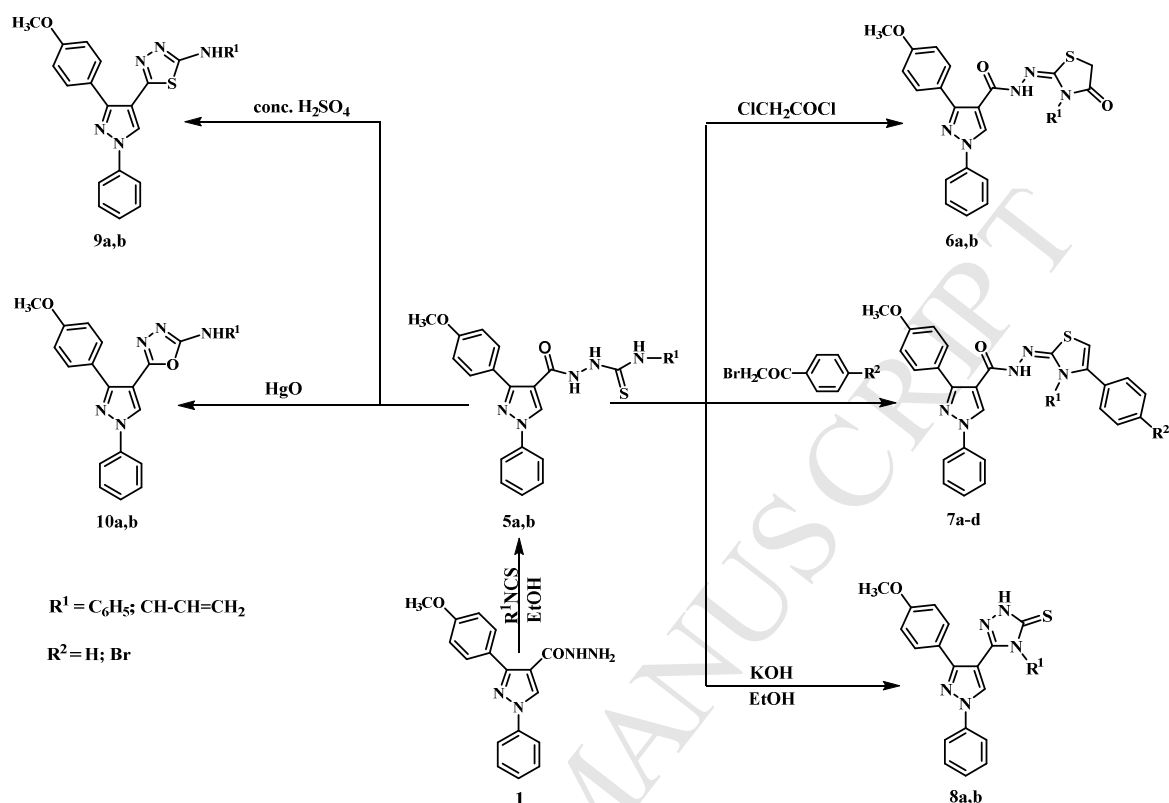
3.1 Chemistry

Target compounds were synthesized according to the steps outlined in **Scheme 1** and **Scheme 2**. The title starting material, acid hydrazide **1**, was prepared by heating the methyl ester with excess amounts of hydrazine hydrate in ethanol, taking into consideration the reaction conditions as reported [31, 32]. In **Scheme 1**, the *N*-formyl derivative **2** was synthesized by heating under reflux acid hydrazide **1** in formic acid [33, 34]. While, the proposed *N*-acetyl derivative **3** was obtained, in excellent yield, by the reaction of acid hydrazide **1** with acetyl chloride in dioxane [35]. Moreover, *N*-arylidinepyrazole-4-carbohydrazides **4a-f** were synthesized by heating under reflux acid hydrazide **1** with different aryl aldehydes [31]. In **Scheme 2**, the key intermediates, substituted thiosemicarbazide **5a,b**, were obtained via heating acid hydrazide **1** with phenyl and allyl isothiocyanate, respectively, in ethanol [35, 36]. Furthermore, they were cyclized into the corresponding thiazolidin-4-one **6a,b** and 3,4-diarylthiazoline **7a-d** derivatives via reaction with chloroacetyl chloride [37, 38] and phenacylbromides [24, 39-41], respectively. In addition, intra-molecular cyclization of substituted thiosemicarbazide **5a,b** under basic, acidic and presence of HgO conditions afforded triazolethione **8a,b**, thiadiazole **9a,b** and oxadiazole **10a,b** derivatives, respectively [35, 42-46]. In the presence bases, the nucleophilicity of the nitrogen atom of NHR group

would increase enough to intramolecularly attack the carbonyl group with simultaneous dehydration [42-45]. In acidic conditions, the nucleophilicity of the nitrogen atom of NHR group would decrease, due to protonation. While, the nucleophilicity of the thiol group would increase enough to intramolecularly attack the carbonyl group, followed by dehydration [44, 47, 48]. In the presence of HgO, the mechanism involved desulfurization, followed by nucleophilic attack of the hydroxyl group on the carbonyl moiety with concurrent dehydration [44, 48, 49].



Scheme 1. Synthetic route of compounds 1-4.



Scheme 2. Synthetic route of compounds **5-10**.

3.1.1 Analytical results

The Results and Discussion of the analytical results is summarized in the Supplementary Material.

3.2 *In silico* experiments

3.2.1 Molecular docking

Antifolates, such as pyrimethamine and cycloguanil are considered as inhibitors of DHFR domain of *Plasmodium falciparum* dihydrofolate reductase thymidylate synthase (*pf* DHFR-TS). This inhibition leads to prevention of DNA synthesis, growth, proliferation and finally parasitic cell death. The resistance to pyrimethamine and its analogues appeared quickly due to site specific amino acid mutation that led to a steric clash between the previous compounds and mutated Asn 108 [12, 13]. On the other hand, the co-crystallized ligand WR99210 has high binding affinity to the mutant *pf* DHFR-TS due to the presence of flexible side chain that adopts a conformation can still fit into the active site modified by mutations [13, 50].

To rationalize the observed *in vitro* antimalarial activity, we explored the binding modes of **4b**, **4c**, **7a** and **7d** in the active site for *pf* DHFR-TS as a putative antimalarial target to our compounds. For this we performed molecular docking experiments on both the wildtype and the quadruple mutant (N51I, C59R, S108N and I164L) *pf* DHFR-TS structures guided by previous studies [51, 52]. Challenging the most active compounds by such highly mutant model would provide clues about the *in silico* affinity of the most active compounds compared to the reference *pf* DHFR-TS binders (e.g., pyrimethamine, cycloguanil and WR99210) especially in a resistant variant of malaria.

Table 1. AutoDock Vina docking scores (kcal mol⁻¹) of the most active compounds along with the reference *pf* DHFR-TS binders (pyrimethamine, cycloguanil and WR99210) bound to the wildtype and quadruple mutant (N51I, C59R, S108N and I164L) *pf* DHFR-TS structures.

Compounds	Docking Score (SD*)	
	Wildtype <i>Pf</i> -DHFR	Quadruple mutant <i>Pf</i> -DHFR
4b	-9.5 (0.06)	-9.5 (0.06)
4c	-9.9 (0)	-10 (0)
7a	-8.1 (0.06)	-9.1 (0.06)
7d	-9 (0.06)	-9.8 (0)
Cycloguanil	-8.8 (0.06)	-7.5 (0)
Pyrimethamine	-8.4 (0)	-7.5 (0)
WR99210	-8.8 (0.06)	-8.8 (0)

*SD is the standard deviation of three consecutive docking runs.

The docking scores of the most active compounds obviously indicated significant *in silico* binding affinities towards both wildtype and mutant *pf* DHFR-TS structures, especially when compared to the reference *pf* DHFR-TS binders (e.g., pyrimethamine, cycloguanil and WR99210) as shown in **Table 1**. Also, the most active compounds exhibited superior docking score towards the mutant *pf* DHFR-TS structure compared to the wildtype, with exception to only **4b** which showed similar scores for both *pf* DHFR-TS structures. This indicates a particular affinity of the most active compounds towards the mutant *pf* DHFR-TS structures and as a possible resistance mechanism of malaria.

The docking pose of **4b** shows favorable interactions in the binding site of wildtype *pf* DHFR-TS as seen in **Figure 3A**. The phenyl pyrazolyl moiety demonstrated favorable hydrophobic contact with the Leu46, Val45 and Ile112. The trimethoxybenzylidene moiety is involved in H-bonding interaction as an acceptor with NH backbone and OH sidechain of Ser120. The *p*-methoxy phenyl group is packed deeply between the co-factor NDP610, Ala16, Cys15, Leu46, Ile164 and Phe58 indicating favorable van der Waal interactions. This binding pose is reproduced upon docking into the quadruple mutant (N51I, C59R, S108N and I164L) *pf*

DHFR-TS structure (**Figure 3B**), however, with the mutant residues appeared to be involved in the interaction pattern. For instance, the mutant Arg59 is observed to show H-bonding interaction with trimethoxybenzylidene moiety of **4b**. In addition, mutant Asn108 and Leu164 appear to surround the *p*-methoxy phenyl group of **4b** via favorable hydrophobic interactions. Likewise, **4c** shows binding mode similar to its congener **4b** for both wildtype and mutant *pf* DHFR-TS structures as shown in **Figure 4**.

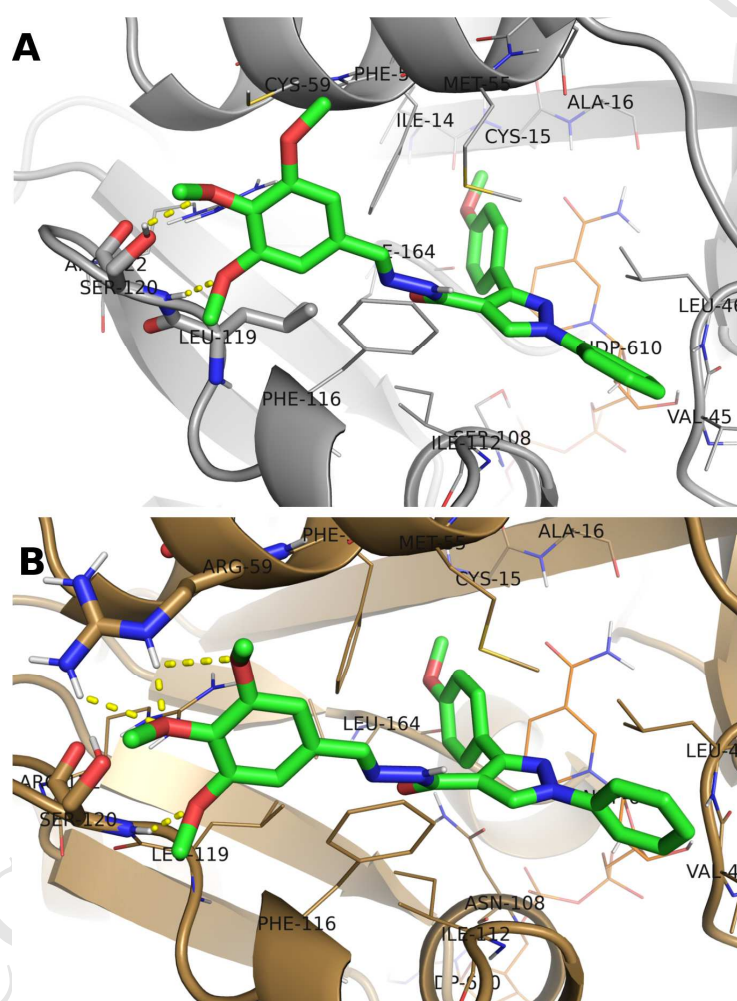


Figure 3. The docking poses of **4b** (green sticks) in the binding site of wildtype *pf* DHFR-TS (PDB code: 1j3i) [53] and quadruple mutant (N51I, C59R, S108N and I164L) *pf* DHFR-TS (PDB code: 1j3k) [53] for (A) and (B), respectively. Yellow-colored dashed lines indicate H-bonding interactions. Non-polar hydrogen atoms were omitted for clarity.

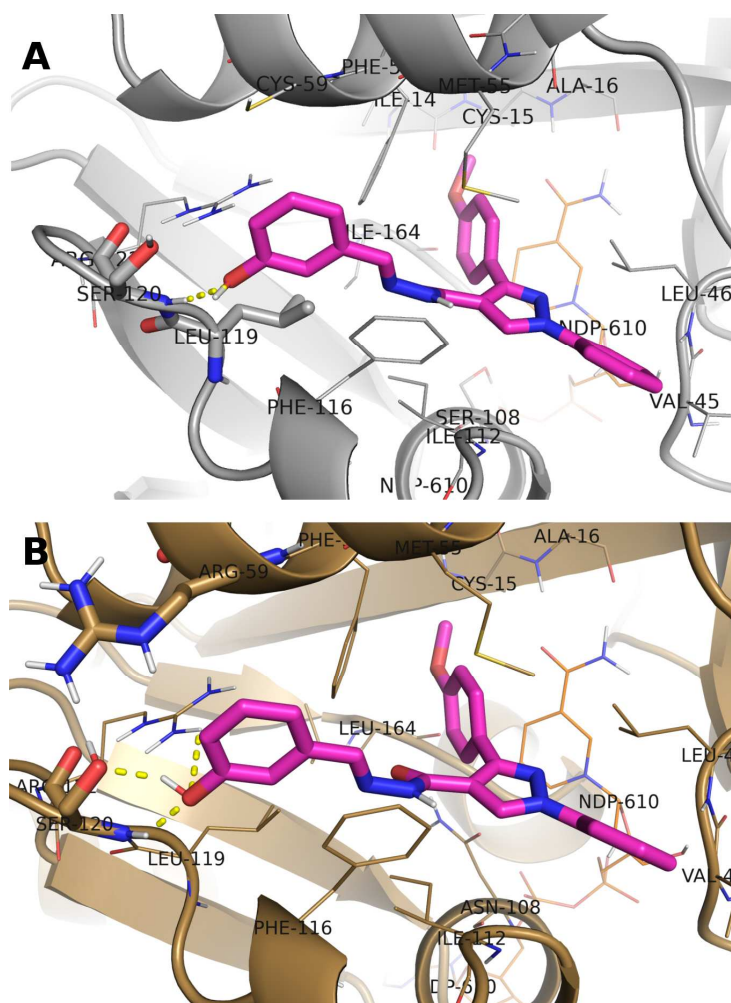


Figure 4. The docking poses of **4c** (purple sticks) in the binding site of wildtype *pf* DHFR-TS (PDB code: 1j3i) and quadruple mutant (N51I, C59R, S108N and I164L) *pf* DHFR-TS (PDB code: 1j3k) for (A) and (B), respectively. Yellow-colored dashed lines indicate H-bonding interactions. Non-polar hydrogen atoms were omitted for clarity.

The postulated binding modes of **7a** and **7d** did not differ dramatically from the predicted poses of **4b** or **4c**, while also some dissimilarity can be observed due to differences of the topological features between **7** and **4** compounds. Taking compound **7a** as an example, the phenyl pyrazolyl moiety of **7a** pose is packed between the side chains of Val45 and Ile46 of the wildtype *pf* DHFR-TS structure, as seen in **Figure 5A**. Like **4b**, the *p*-methoxyphenyl group of **7a** is packed deeply between the co-factor NDP610, Ala16, Cys15, Leu46, Ile164 and Phe58. Also, the diphenylthiazolylidene moiety of **7a** appeared to be packed between the side chains of Met55, Cys59, Phe116, Arg122 and Cys59. Again, this postulated binding pose did not differ intensely from the docked pose into the quadruple mutant (N51I, C59R, S108N and I164L) *pf* DHFR-TS structure, as shown in **Figure 5B**. The mutant Arg59 is in a close

proximity to the diphenylthiazolylidene indicating a favorable cation- π interaction of the protonated guanidino group of the residue with the aromatic group *N*-phenylthiazolyl group of **7a**. In addition, like **4b** and **4c**, Asn108 and Leu164 are observed to border the *p*-methoxy phenyl group of **7a** via favorable hydrophobic interactions.

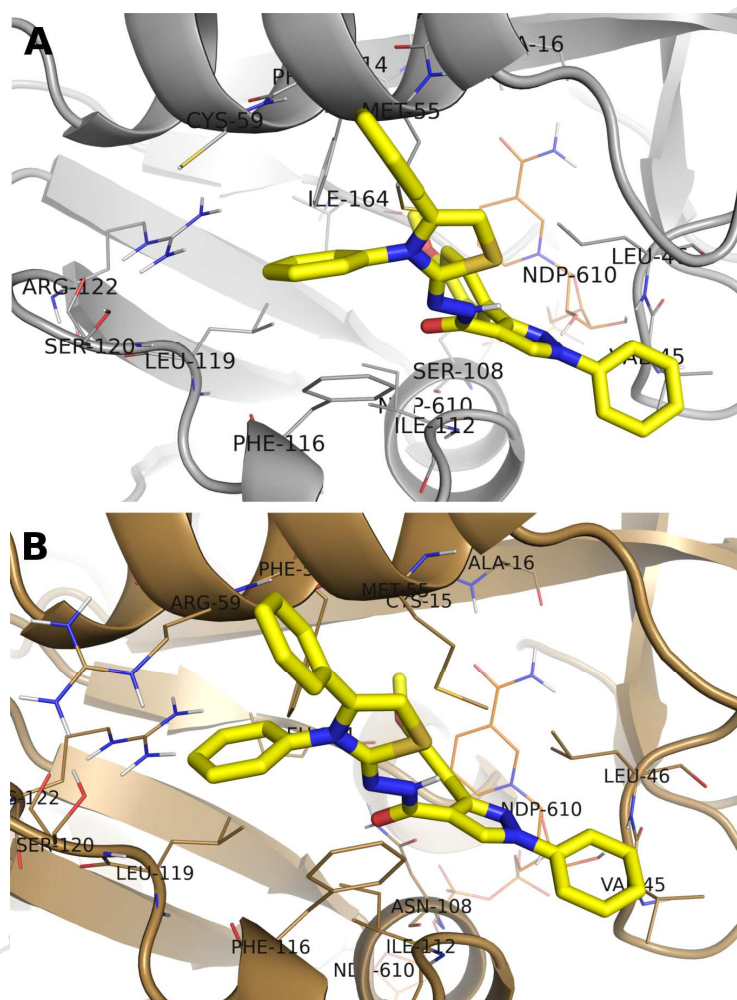


Figure 5. The docking poses of **7a** (yellow sticks) in the binding site of wildtype *pf* DHFR-TS (PDB code: 1j3i) and quadruple mutant (N51I, C59R, S108N and I164L) *pf* DHFR-TS (PDB code: 1j3k) for (A) and (B), respectively. Yellow-colored dashed lines indicate H-bonding interactions. Non-polar hydrogen atoms were omitted for clarity.

3.2.2 *In silico* prediction of physicochemical properties, pharmacokinetic, drug likeness score and toxicity profile

The Results and Discussion of this section is summarized in the Supplementary Material.

3.3 Biological screening

3.3.1 *In vivo* antimalarial activity testing against *P. berghei*

All the newly synthesized compounds were screened for their *in vivo* antimalarial activity using a 4-day suppressive test in *P. berghei* infected mice at a dose of 48.4 $\mu\text{mol/Kg/day}$ [54], **Table 2**.

Table 2: *In vivo* antimalarial activity of the newly synthesized compounds against *P. berghei* at dose 48.4 $\mu\text{M/kg/day}$.

Compound Number	% Parasitemia*	% Suppression	Mean survival time (days)*
2	26 \pm 1.6	70.11	6.66 \pm 0.2
3	32 \pm 2.8	63.21	6.66 \pm 0.4
4a	13 \pm 0.4	85.05	9.33 \pm 0.2
4b	6\pm0.6	93.10	ND**
4c	2\pm0.4	97.70	ND**
4d	14 \pm 0.6	67.81	10.50 \pm 0.4
4	12 \pm 0.6	86.20	11.50 \pm 0.3
4f	18 \pm 0.2	79.31	8.83 \pm 0.3
5a	23 \pm 0.6	73.56	6.66 \pm 0.5
5b	26 \pm 1.2	70.11	6.66 \pm 0.3
6a	15 \pm 0.8	82.75	12.83 \pm 0.5
6b	18 \pm 1.4	79.31	11.33 \pm 0.4
7a	2\pm0.4	97.70	ND**
7b	16 \pm 0.6	81.60	11.66 \pm 0.2
7c	25 \pm 0.8	71.26	7.33 \pm 0.3
7d	8\pm0.2	90.80	ND**
8a	23 \pm 0.6	73.56	7.66 \pm 0.6
8b	32 \pm 1.8	63.21	5.50 \pm 0.2
9a	24 \pm 0.2	72.21	7.16 \pm 0.4
9b	22 \pm 0.4	74.71	8.33 \pm 0.6
10a	13 \pm 0.8	85.05	11.16 \pm 0.2
10b	27 \pm 0.6	68.96	7.33 \pm 0.4
Control	87\pm1.2	0.00	4.33\pm0.7
Pyrimethamine	0.0	100	ND**
Chloroquine phosphate	0.0	100	12.22\pm0.2

* Values are M±SD, P< 0.05

**

ND: No death recorded during experimental period

3.3.1.1 Structure activity relationship

At a certain stage of the design of this work, hydrazone derivatives were prepared by condensation of acid hydrazide derivative **1** with different aryl/heterylaldehydes. Molecular modeling of the proposed compounds showed formation of different hydrogen bonds with amino acid residues in the active site of *pfDHFR*-TS. The results of *in vivo* antimalarial screening of *N*-arylhyazone **4b** is in coherence with the rational concluded from the docking experiment since emphasizing the high activity against *P. berghei*. On the other hand, introduction of halogens in *N*-arylhyazone derivative **4d** slightly decreased their activity. This could be attributed to the lower solubility rate of these compounds. Moreover, condensation of acid hydrazide **1** with thiophene-2-carboxaldehyde resulted in thiophene derivative **4e** displaying good anti-plasmodial activity against *P. berghei*. This could be due to the increased hydrophobicity of these compounds. The highest antimalarial activity of schiff base **4c** could be attributed to its interaction similarity with the backbone of target enzyme *pfDHFR*-TS, similar to that of the co-crystalized ligand. Additionally, its solubility increased, due to the presence of hydroxyl group. In a trial to increase the activity of the synthesized compounds, hybridization of pyrazole ring with thiazolidinone or thiazole ring through three atom spacer to produce **6a,b** and **7a-d**, respectively, was achieved. In general, thiazole derivatives **7a-d** showed higher activity than thiazolidinone derivatives **6a,b**. Moreover, compound **7a** displayed the highest percentage of suppression, 97.0%, compared with other thiazole derivatives. Direct attachment of different heterocyclic rings to the parent pyrazole moiety resulted in compounds having variable antimalarial activity profile. Therefore, cyclization of thiosemicarbazides **5a,b** showed different effects on the activity of corresponding derivatives. For example, higher activity was associated with formation of oxadiazole derivative **10a** and thiadiazole **9b**. Besides, no change in the activity was attributed to triazole derivatives **8a**, and a decrease in the activity of **8b**, **9a** and **10b** was clear.

3.3.2 In vitro antimalarial activity testing against *P. falciparum*

The compounds most active against *P. berghei*, compounds **4b**, **4c**, **7a** and **7d**, were screened for their *in vitro* antimalarial activity against chloroquine resistant strain *P. falciparum* (RKL9) using the standard method described by Trager and Jensen [55] (Table 3).

Table 3: *In vitro* antimalarial activity of the most active compounds against chloroquine-resistant strain *P. falciparum* (RKL9).

Comp No.	IC ₅₀ μM±SD*
4b	0.0398±0.004

4c	0.0142±0.002
7a	0.0492±0.014
7d	0.0319±0.002
Chloroquine phosphate	0.1930±0.003
Pyrimethamine	0.01246±0.002

*Results of two separate determinations.

3.3.2.1 Structure activity relationship

Results of *in vitro* antiplasmodial screening showed that all test compounds displayed higher antimalarial activity than the standard chloroquine phosphate against chloroquine-resistant *P. falciparum* (RKL9). It is worth mentioning that *m*-hydroxy benzylidenehydrazone derivative **4c** was the most potent with IC₅₀ = 0.0142 μM. This is in agreement with the previously mentioned results of the *in vivo* antimalarial screening against *P. berghei*.

3.3.3 Toxicity studies

3.3.3.1 Lysosomal anti-inflammatory activity and hemolytic effect on RBCs

Lysosomal anti-inflammatory activity and hemolytic effect on RBCs of the most active antimalarial compounds were evaluated according to Chatterjee *et al* [56] and Evans *et al* [57] (Table 4). It was noticeable that compound **7a** was the most potent anti-inflammatory with IC₅₀ 71-fold higher than IC₅₀ of the corresponding antimalarial activity. It also displayed the least hemolytic effect, even at very high concentrations. While, compound **4b** was the least active anti-inflammatory and most toxic derivative, with IC₅₀ 1700-fold higher than IC₅₀ corresponding to the antimalarial activity.

Table 4: RBCs hemolysis assay of the most active antimalarial compounds.

Cpd No.	Anti-inflammatory%			IC ₅₀ μg/ml	IC ₅₀ (μM)	Antihemolytic %			IC ₅₀ μg/ml	IC ₅₀ (μM)
	5 (μg/ml)	20 (μg/ml)	40 (μg/ml)			5 (μg/ml)	20 (μg/ml)	40 (μg/ml)		
4b	29.69±2.5 at 10.28 μM	17.52±0.35 at 41.13 μM	5.34±0.6 at 82.27 μM	25.50±1.1	52.45±2.3	41±1.3 at 10.28 μM	85 ±3.5 at 41.13 μM	97.8±6.3 at 82.27 μM	58.75 ±2.5	120.8±5.1
4c	49.03 ±3.2 at 12.12 μM	54.31±2.5 at 48.49 μM	59.58±6.7 at 96.98 μM	6.60±0.9	16±2.2	32±1.02 at 12.12 μM	40±2.1 at 48.49 μM	44±2.03 at 96.98 μM	54.71 ±4.9	132.6±11.8
7a	56.11±1.6 at 9.19 μM	81.19 at ±3.7 36.78 μM	106.28 ±3.8 at 73.58 μM	1.90±0.2	3.49±0.37	41±1.91 at 9.19 μM	79±3.0 5 at 36.78 μM	99.8±5.81 at 73.58 μM	75.15 ±3.6	138.03 ±6.6

	μM		μM				μM	μM		
7d	35.23±0.94 at 8.52 μM	57.79±2.1 at 34.10 μM	80.34±1.3 at 68.20 μM	7.90±0.5	13.74±0.85	16±0.06 at 8.52 μM	59±4.0 at 34.10 μM	68±5.02 at 68.20 μM	46.64 ±5.7	79.52±9.03

3.3.3.2 White blood cell cytotoxicity assessment

The effect of different concentrations of test compounds on proliferation of normal peripheral blood mono nuclear cells (PBMC) was determined in order to measure their safety (**Table 5**). Neutral red uptake assay was performed as the amount of retained dye is directly proportional to the number of viable cells with an intact membrane [58]. It was noticeable that compound **4c** was the least toxic derivative, displaying the highest IC_{50} value equal to 1000.18 μM . This IC_{50} was 70000-fold higher than IC_{50} related to the antimalarial activity. Additionally, compound **4b** was considered the most toxic compound as it showed the least IC_{50} value. However, this IC_{50} was 783-fold higher than IC_{50} of the antimalarial activity.

Table 5: cytotoxicity assessment of test compounds on normal peripheral blood mono nuclear cells (PBMC).

Comp No.	6.25 ($\mu\text{g/ml}$)	25 ($\mu\text{g/ml}$)	100 ($\mu\text{g/ml}$)		IC_{50} ($\mu\text{g/ml}$)	IC_{50} (μM)
4b	43.00±1.9	60.00±2.3	77.93±2.9	$y = 0.3344x + 45.678$	15.15±0.02	31.16±0.041
4c	- 19.18±0.3	54.42±1.8	12.78±0.21	$y = 0.0849x + 12.293$	420.00±12.1	1000.18±30.2
7a	-6.20±0.4	1.63±0.06	48.27±1.3	$y = 0.5989x - 12.178$	103.34±5.2	190.02±9.6
7d	8.46±0.9	16.05±0.9	39.93±1.3	$y = 0.3307x + 7.01$	130.30±3.2	222.16±5.5

3.3.3.3 In vivo acute toxicity testing

The most active antiplasmodial compounds **4b**, **4c**, **7a** and **7d** were evaluated for their acute toxicity in mice. The absence of any toxicity signs, difference in the weight of the mice and death cases were recorded during 3 days of observation post administration of the test compounds. Thus, it could be concluded that the test compounds were non-toxic and well tolerated by the experimental animals orally up to 150 mg/kg. In addition, evaluation of their toxicity through the parenteral route was performed and the results revealed that all the selected test compounds were non-toxic up to 75 mg/kg.

4 Conclusion

New 1,3,4-trisubstituted pyrazole derivatives were synthesized and biologically evaluated for their antiplasmodial activity. All synthesized compounds were evaluated for their *in vivo* antimalarial activity using a 4-day suppressive test using Swiss Albino mice infected with *P. berghei* ANKA strain. It is worth mentioning that compounds **4b**, **4c**, **7a** and **7d** displayed the highest percent of suppression, above 90%, among all test compounds. These compounds were further subjected to *in vitro* antiplasmodial testing against chloroquine-resistant *P. falciparum* strain RKL9 using chloroquine phosphate as a reference drug. All compounds showed inhibitory effects higher than chloroquine and compound **4c** was found to be the most potent with $IC_{50} = 0.0142 \mu\text{M}$. **4b**, **4c**, **7a** and **7d** were docked into the active site of the wildtype and quadruple mutant (N51I, C59R, S108N and I164L) *pf* DHFR-TS to rationalize their observed antimalarial activities. In addition, these compounds were subjected to *in silico* prediction of physicochemical properties and pharmacokinetic profiles. They showed reasonable drug-likeness scores, as well as pharmacokinetic properties. Other important issues, such as compliance with Lipinski's rule of five, acceptable cell permeability through Caco-2 model and low toxicity profile advocated these compounds to be drug-like candidates.

In addition, toxicity studies on the most active antimalarial compounds were performed. It was found that compound **7a** was the most potent anti-inflammatory and safe derivative with IC_{50} 71-fold higher than IC_{50} related to the antimalarial activity. Moreover, cytotoxicity assessment revealed that compound **4c** was the least toxic derivative with IC_{50} 70000-fold higher than IC_{50} related to the antimalarial activity. At the least, acute toxicity studies showed that all tested compounds were non-toxic and well-tolerated up to 150 mg/kg via oral route and 75 mg/kg via parenteral route.

5 Experimental:

5.1 Chemistry

Melting points were determined in open-glass capillaries using a Griffin melting point apparatus and all were uncorrected. Infrared spectra (IR) were recorded using KBr discs, on Perkin-Elmer 1430 infrared spectrophotometer. Proton and carbon nuclear magnetic resonance spectra ($^1\text{H-NMR}$ & $^{13}\text{C-NMR}$) were scanned on Joel-500 MHz, Bruker-400 MHz and mercury-300 MHz NMR-spectrometer (DMSO- d_6 & CDCl_3). Chemical shifts were given in δ (ppm) using tetramethylsilane (TMS) as internal standard. Microanalyses were performed on elemental analyzer at The Regional Center for Mycology and Biotechnology. Following up of the reactions rates was performed by thin-layer chromatography (TLC) on ready-made silica sheets and the spots were visualized by exposure to iodine vapors or UV-lamp at $\lambda = 254 \text{ nm}$. Electron impact mass spectra (EIMS) were run on a gas chromatograph/mass spectrometer at

The Regional Center for Mycology and Biotechnology and relative intensity percentage corresponding to the most characteristic fragments was recorded.

5.1.1 General method for preparation of 3-(4-Methoxyphenyl)-1-phenyl-1H-pyrazole-4-carboxylic acid hydrazide 1 [31, 32]

To a suspension of pyrazole-4-carboxylic acid methyl ester (1.54 g, 5 mmol) in absolute ethanol (10 ml), excess hydrazine hydrate (10 ml) was added. The reaction mixture was stirred for 24 h at room temperature. Then the solvent was evaporated and the residue washed with water, filtered, dried, and crystallized from ethanol as white solid, mp 158-160 °C (Reported, 157-158 °C [31]), in yield (97.5%). IR (cm⁻¹): 3470, 3312 (NH₂); 3206 (NH); 1649 (C=O); 1617 (C=N).

5.1.2 General method for preparation of N'-Formyl-3-(4-methoxyphenyl)-1-phenyl-1H-pyrazole-4-carbohydrazide 2

A solution of acid hydrazide **1** (0.3 g, 1 mmol) in formic acid (2 ml) was heated under reflux for 6 h. After cooling, the reaction mixture was concentrated and the residue obtained was filtered, washed, dried and crystallized from methanol as off-white crystals, mp 170-172 °C, in yield (82%). IR (cm⁻¹): 3310, 3215 (NH); 1715 (CHO); 1643 (amidic C=O); 1611 (C=N). ¹H-NMR (DMSO-d₆, δ ppm): 3.79 (s, 3H, OCH₃); 6.95, 7.01 (2d, *J* = 8.7 Hz, 2H, methoxy phenyl-C_{3,5}-H); 7.36-7.40 (m, 1H, phenyl-C₄-H); 7.52-7.57 (m, 1H, phenyl-C_{3,5}-H); 7.4, 7.81 (2d, *J* = 8.7 Hz, 2H, methoxyphenyl-C_{2,6}-H); 7.83, 7.98 (2d, *J* = 8.7 Hz, 2H, phenyl-C_{2,6}-H); 9.16 (s, 1H, NH, D₂O-exchangeable); 9.24 (s, 1H, pyrazole-C₅-H); 9.27 (s, 1H, CHO); 11.34 (s, 1H, NH, D₂O-exchangeable). ¹³C-NMR (DMSO-d₆, δ ppm): 55.76 (OCH₃); 105.79 (pyrazole-C₄); 114.23 (methoxyphenyl-C_{3,5}); 119.49 (phenyl-C_{2,6}); 124.32 (methoxy phenyl-C₁); 127.89 (phenyl-C₄); 130.19 (methoxyphenyl-C_{2,6}); 130.52 (phenyl-C_{3,5}); 131.72 (pyrazole-C₅); 139.27 (phenyl-C₁); 151.03 (pyrazole-C₃); 154.29 (methoxyphenyl-C₄); 159.69 (amidic C=O), 160.37 (CHO). Elemental analysis Calcd for C₁₈H₁₆N₄O₃: C, 64.28; H, 4.79; N, 8.80. Found: C, 64.57; H, 4.83; N, 16.92.

5.1.3 General method for preparation of N'-Acetyl-3-(4-methoxyphenyl)-1-phenyl-1H-pyrazole-4-carbohydrazide 3

To a solution of acid hydrazide **1** (0.3 g, 1 mmol) in dioxane (10 ml), acetyl chloride (0.07 ml, 1 mmol) was added. The reaction mixture was heated under reflux for 6 h, then the solvent was removed and the residue was triturated with an ice-H₂O mixture. The product formed was filtered, washed with H₂O, dried and crystallized from methanol as yellow crystals, mp 130-132 °C, in yield (83%). IR (cm⁻¹): 3244, 3128 (NH); 1725 (CH₃CO); 1692 (amidic C=O); 1608 (C=N). ¹H-NMR (CDCl₃, δ ppm): 2.33 (s, 3H, CH₃); 3.78 (s, 3H, OCH₃); 6.94 (d, *J* =

8.8 Hz, 2H, methoxyphenyl-C_{3,5}-H); 7.28 (t, $J = 7.4$ Hz, 1H, phenyl-C₄-H); 7.38-7.42 (m, 3H, phenyl-C_{3,5}-H and NH); 7.64-7.66 (m, 5H, methoxyphenyl-C_{2,6}-H and phenyl-C_{2,6}-H and NH); 8.49 (s, 1H, pyrazole-C₅-H). ¹³C-NMR (CDCl₃, δ ppm): 25.09 (CH₃); 55.41 (OCH₃); 114.52 (pyrazole-C₄); 114.74 (methoxyphenyl-C_{3,5}); 119.60 (phenyl-C_{2,6}); 124.00 (methoxyphenyl-C₁); 127.72 (phenyl-C₄); 129.65 (methoxyphenyl-C_{2,6}); 130.72 (phenyl-C_{3,5}); 131.99 (pyrazole-C₅); 139.07 (phenyl-C₁); 151.53 (pyrazole-C₃); 160.72 (methoxyphenyl-C₄); 163.21 (amidic C=O); 171.67 (CH₃CO). Elemental analysis Calcd for C₁₉H₁₈N₄O₃: C, 65.13; H, 5.18; N, 15.99. Found: C, 65.37; H, 5.16; N, 16.25.

5.1.4 General method for preparation of *N'*-arylidene-3-(4-methoxyphenyl)-1-phenyl-1H-pyrazole-4-carbohydrazide 4a-f

A mixture of acid hydrazide **1** (0.3 g, 1 mmol) and appropriate aldehyde (1 mmol) in absolute ethanol (10 ml) was heated under reflux for 1-3 h. The precipitate formed was filtered, washed with ethanol, dried and crystallized from ethanol as white solid.

5.1.4.1 *N'*-benzylidene-3-(4-methoxyphenyl)-1-phenyl-1H-pyrazole-4-carbohydrazide 4a

The product was obtained as white solid, mp 242-244 °C, in yield (89%). IR (cm⁻¹): 3190 (NH); 1646 (C=O); 1605 (C=N). ¹H-NMR (DMSO-d₆, δ ppm): 3.80 (s, 3H, OCH₃); 7.00 (d, $J = 8.7$ Hz, 2H, methoxyphenyl-C_{3,5}-H); 7.36-7.45 (m, 5H, *N*-phenyl-C_{3,4,5}-H and phenyl-C_{3,5}-H); 7.54-7.71 (m, 3H, *N*-phenyl-C_{2,6}-H and phenyl-C₄-H); 7.83 (d, $J = 8.7$ Hz, 2H, methoxyphenyl-C_{2,6}-H); 7.92 (d, $J = 7.5$ Hz, 2H, phenyl-C_{2,6}-H); 8.29 (s, 1H, pyrazole-C₅-H); 8.99 (s, 1H, -CH=N); 11.68 (s, 1H, NH, D₂O-exchangeable). Elemental analysis Calcd for C₂₄H₂₀N₄O₂: C, 72.71; H, 5.08; N, 14.13. Found: C, 72.98; H, 5.16; N, 14.37.

5.1.4.2 3-(4-Methoxyphenyl)-1-phenyl-*N'*-(3,4,5-trimethoxybenzylidene)-1H-pyrazole-4-carbohydrazide 4b

The product was obtained as white solid, mp 232-234 °C, in yield (77%). IR (cm⁻¹): 3166 (NH); 1661 (C=O); 1643, 1605 (C=N). ¹H-NMR (DMSO-d₆, δ ppm): 3.71 (1s, 3H, OCH₃); 3.80 (1s, 3H, OCH₃); 3.84 (1s, 6H, 2 OCH₃); 7.01 (d, $J = 8.25$ Hz, 2H, methoxyphenyl-C_{3,5}-H); 7.08 (s, 2H, tri methoxyphenyl-C_{2,6}-H); 7.38 (t, $J = 7.35$ Hz, 1H, phenyl-C₄-H); 7.54-7.59 (m, 2H, phenyl-C_{3,5}-H); 7.83 (d, $J = 8.25$ Hz, 2H, methoxyphenyl-C_{2,6}-H); 7.92 (d, $J = 7.8$ Hz, 2H, phenyl-C_{2,6}-H); 8.22 (s, 1H, pyrazole-C₅-H); 8.99 (s, 1H, -CH=N); 11.68 (s, 1H, NH, D₂O-exchangeable). Elemental analysis Calcd for C₂₇H₂₆N₄O₅: C, 66.65; H, 5.39; N, 11.52. Found: C, 66.91; H, 5.45; N, 11.78.

5.1.4.3 *N'*-(3-Hydroxybenzylidene)-3-(4-methoxyphenyl)-1-phenyl-1H-pyrazole-4-carbohydrazide 4c

The product was obtained as white solid, mp 219-220 °C, in yield (68%). IR (cm⁻¹): 3419 (OH); 3204 (NH); 1662 (C=O); 1634, 1600 (C=N). ¹H-NMR (DMSO-d₆, δ ppm): 3.80 (s, 3H, OCH₃); 6.82 (d, $J = 8.7$ Hz, 1H, hydroxyphenyl-C₄-H); 7.00 (d, $J = 9$ Hz, 2H, methoxyphenyl-

C_{3,5}-H); 7.08-7.25 (m, 3H, hydroxyphenyl-C_{2,5,6}-H); 7.38 (t, $J = 7.35$ Hz, 1H, phenyl-C₄-H); 7.54-7.59 (m, 2H, phenyl-C_{3,5}-H); 7.83 (d, $J = 9$ Hz, 2H, methoxyphenyl-C_{2,6}-H); 7.92 (d, $J = 7.8$ Hz, 2H, phenyl-C_{2,6}-H); 8.19 (s, 1H, pyrazole-C₅-H); 8.99 (s, 1H, -CH=N); 9.6 (s, 1H, OH, D₂O-exchangeable); 11.99 (s, 1H, NH, D₂O-exchangeable). Elemental analysis Calcd for C₂₄H₂₀N₄O₃: C, 69.89; H, 4.89; N, 13.58. Found: C, 70.12; H, 4.96; N, 13.79.

5.1.4.4 *N'*-(4-Fluorobenzylidene)-3-(4-methoxyphenyl)-1-phenyl-1H-pyrazole-4-carbohydrazide 4d

The product was obtained as white solid, mp 223-225 °C, in yield (66%). IR (cm⁻¹): 3185 (NH); 1660 (C=O); 1603 (C=N). ¹H -NMR (300 MHz, DMSO-d₆, δ ppm): 3.80 (s, 3H, OCH₃); 7.00 (d, $J = 8.7$ Hz, 2H, methoxyphenyl-C_{3,5}-H); 7 (m, 2H, fluorophenyl-C_{3,5}-H); 7.38 (t, $J = 7.35$ Hz, 1H, phenyl-C₄-H); 7.54-7.59 (m, 2H, phenyl-C_{3,5}-H); 7.8-7.84 (m, 4H, methoxyphenyl-C_{2,6}-H and fluorophenyl-C_{2,6}-H); 7.92 (d, $J = 7.8$ Hz, 2H, phenyl-C_{2,6}-H); 8.29 (s, 1H, pyrazole-C₅-H); 8.99 (s, 1H, -CH=N); 11.77 (s, 1H, NH, D₂O-exchangeable). EIMS m/z (% relative abundance): 415 (4) (M⁺+1), 414 (12) (M⁺), 293 (16), 278 (20), 277 (100), 234 (5), 145 (6), 104 (9), 77 (16), 75 (21). Elemental analysis Calcd for C₂₄H₁₉FN₄O₂: C, 69.55; H, 4.62; N, 13.52. Found: C, 69.81; H, 4.67; N, 13.74.

5.1.4.5 3-(4-Methoxyphenyl)-1-phenyl-*N'*-(thiophen-2-ylmethylene)-1H-pyrazole-4-carbohydrazide 4e

The product was obtained as white solid, mp 213-215 °C, in yield (62%). IR (cm⁻¹): 3173 (NH); 1654 (C=O); 1600 (C=N); 1058 (C-S-C). ¹H -NMR (DMSO-d₆, δ ppm): 3.80 (s, 3H, OCH₃); 7.00 (d, $J = 8.25$ Hz, 2H, methoxyphenyl-C_{3,5}-H); 7.13 (m, 1H, thiophen-C₄-H); 7.42 (t, $J = 7.35$ Hz, 1H, phenyl-C₄-H); 7.46-7.67 (m, 4H, phenyl-C_{3,5}-H, thiophen-C_{3,5}-H); 7.82 (d, $J = 8.25$ Hz, 2H, methoxyphenyl-C_{2,6}-H); 7.92 (d, $J = 7.7$ Hz, 2H, phenyl-C_{2,6}-H); 8.50 (s, 1H, pyrazole-C₅-H); 8.96 (s, 1H, -CH=N); 11.64 (s, 1H, NH, D₂O-exchangeable). Elemental analysis Calcd for C₂₂H₁₈N₄O₂S: C, 65.65; H, 4.51; N, 13.92; S, 7.97. Found: C, 65.89; H, 4.54; N, 14.15; S, 8.04.

5.1.4.6 3-(4-Methoxyphenyl)-1-phenyl-*N'*-(pyridin-4-ylmethylene)-1H-pyrazole-4-carbohydrazide 4f

The product was obtained as white solid, mp 198-200 °C, in yield (70%). IR (cm⁻¹): 3181 (NH); 1664 (C=O); 1590 (C=N). ¹H -NMR (DMSO-d₆, δ ppm): 3.78 (s, 3H, OCH₃); 6.98 (d, $J = 8.7$ Hz, 2H, methoxyphenyl-C_{3,5}-H); 7.37 (m, 1H, phenyl-C₄-H); 7.53-7.65 (m, 4H, phenyl-C_{2,3,5,6}-H); 7.79 (d, $J = 8.7$ Hz, 2H, methoxyphenyl-C_{2,6}-H); 7.90 (d, $J = 8.7$ Hz, 2H, pyridine-C_{2,6}-H); 8.26 (s, 1H, pyrazole-C₅-H); 8.63 (d, $J = 8.7$ Hz, pyridine-C_{2,6}-H); 9.02 (s, 1H, -CH=N); 11.99 (s, 1H, NH, D₂O-exchangeable). ¹³C-NMR (DMSO-d₆, δ ppm): 55.70 (OCH₃); 114.15 (methoxyphenyl-C_{3,5} and pyrazole-C₄); 119.21 (phenyl-C_{2,6}); 121.49 (pyridine-C_{2,6}); 125.32 (methoxyphenyl-C₁); 127.60 (phenyl-C₄); 130.06 (methoxy phenyl-C_{2,6}); 130.29 (phenyl-C_{3,5}); 131.26 (pyrazole-C₅); 139.50 (phenyl-C₁); 144.77 (pyridine-C₁); 146.80

(CH=N); 150.82 (pyridine-C_{3,5} and pyrazole-C₃); 160.07 (methoxy phenyl-C₄); 161.00 (C=O). Elemental analysis Calcd for C₂₃H₁₉N₅O₂: C, 69.51; H, 4.82; N, 17.62. Found: C, 69.82; H, 4.88; N, 17.89.

5.1.5 General method for preparation of 2-[3-(4-Methoxyphenyl)-1-phenyl-1H-pyrazole-4-carbonyl]-N-(phenyl/allyl)hydrazine-carbothioamides 5a,b

A suspension of acid hydrazide **1** (0.3 g, 1 mmol) and isothiocyanate (1 mmol) in absolute ethanol (10 ml) was heated under reflux for 4 h and then cooled to room temperature. The precipitate formed was filtered, washed with ethanol, dried and crystallized from ethanol.

5.1.5.1 2-[3-(4-Methoxyphenyl)-1-phenyl-1H-pyrazole-4-carbonyl]-N-phenylhydrazinecarbo-thioamide 5a

The product was obtained as white solid, mp 183-185°C, in yield (85%). IR (cm⁻¹): 3411, 3328, 3132 (NH); 1674 (C=O); 1601 (C=N); 1531, 1250, 1224 and 966 (N-C=S I, II, III and IV bands, respectively). ¹H-NMR (DMSO-d₆, δ ppm): 3.77 (s, 3H, OCH₃); 6.95 (d, *J* = 8.4 Hz, 2H, methoxyphenyl-C_{3,5}-H); 7.15 (t, *J* = 7.25 Hz, 1H, NH-phenyl-C₄-H); 7.31-7.43 (m, 5H, phenyl-C_{3,4,5}-H and NH-phenyl-C_{3,5}-H); 7.54-7.57 (m, 2H, NH-phenyl-C_{2,6}-H); 7.18 (d, *J* = 8.4 Hz, 2H, methoxyphenyl-C_{2,6}-H); 7.85 (d, *J* = 7.65 Hz, 2H, phenyl-C_{2,6}-H); 9.00 (s, 1H, pyrazole-C₅-H); 9.70 (s, 1H, NH, D₂O-exchangeable); 9.75 (s, 1H, S=C-NH, D₂O-exchangeable); 10.25 (s, 1H, O=C-NH, D₂O-exchangeable). ¹³C-NMR (DMSO-d₆, δ ppm): 55.70 (OCH₃); 113.92 (methoxyphenyl-C_{3,5}); 114.99 (pyrazole-C₄); 119.17 (phenyl-C_{2,6}); 124.97 (NH-phenyl-C_{2,6}); 125.82 (methoxy phenyl-C₁); 126.63 (phenyl-C₄); 127.69 (NH-phenyl-C₄); 128.63 (NH-phenyl-C_{3,5}); 130.42 (methoxyphenyl-C_{2,6} and pyrazole-C₅); 130.52 (phenyl-C_{3,5}); 139.46 (NH-phenyl-C₁); 139.67 (phenyl-C₁); 152.21 (pyrazole-C₃); 160.05 (methoxyphenyl-C₄); 163.50 (C=O); 170.02 (C=S). Elemental analysis Calcd for C₂₄H₂₁N₅O₂S: C, 64.99; H, 4.77; N, 15.79; S, 7.23. Found: C, 65.23; H, 4.81; N, 15.94; S, 7.41.

5.1.5.2 N-Allyl-2-[3-(4-methoxyphenyl)-1-phenyl-1H-pyrazole-4-carbonyl]hydrazinecarbothioamide 5b

as white solid, mp 132-134°C, in yield (90%). IR (cm⁻¹): 3326, 3220, 3129 (NH); 1668 (C=O); 1616 (C=N); 1541, 1249, 1225 and 959 (N-C=S I, II, III and IV bands, respectively). ¹H-NMR (DMSO-d₆, δ ppm): 3.81 (s, 3H, OCH₃); 4.15 (d, *J* = 5.2 Hz, 2H, CH₂=CH-CH₂-); 5.07 (d, *J* = 10.4 Hz, 1H, H_{cis}-CH₂=CH-CH₂-); 5.15 (d, *J* = 17.2 Hz, 1H, H_{trans}-CH₂=CH-CH₂-); 5.84-5.90 (m, 1H, CH₂=CH-CH₂-); 6.97 (d, *J* = 8.4 Hz, 2H, methoxyphenyl-C_{3,5}-H); 7.41 (t, *J* = 7.6 Hz, 1H, phenyl-C₄-H); 7.57-7.61 (m, 2H, phenyl-C_{3,5}-H); 7.83-7.86 (m, 4H, methoxyphenyl-C_{2,6}-H and phenyl-C_{2,6}-H); 8.24 (s, 1H, NH, D₂O-exchangeable); 8.97 (s, 1H, pyrazole-C₅-H); 9.42 (s, 1H, S=C-NH, D₂O-exchangeable); 10.07 (s, 1H, O=C-NH, D₂O-exchangeable). Elemental analysis Calcd for C₂₁H₂₁N₅O₂S: C, 61.90; H, 5.19; N, 17.19; S, 7.87. Found: C, 62.21; H, 5.24; N, 17.38; S, 7.94.

5.1.6 General method for preparation of 3-(4-Methoxyphenyl)-N'-[4-oxo-3-(phenyl/allyl)thiazolidin-2-ylidene]-1-phenyl-1H-pyrazole-4-carbohydrazides 6a,b

A mixture of substituted thiosemicarbazide **5a** or **5b** (1 mmol) and chloroacetyl chloride (0.08 ml, 1 mmol) in dry dioxane (10 ml) was heated under reflux for 8 h. After cooling, the precipitate formed was washed with ethanol, filtered, washed again with H₂O, dried and crystallized from appropriate solvents.

5.1.6.1 3-(4-Methoxyphenyl)-N'-(4-oxo-3-phenylthiazolidin-2-ylidene)-1-phenyl-1H-pyrazole-4-carbohydrazide 6a

The product was crystallized from chloroform as yellow crystals, mp 156-158 °C, in yield (55%). IR (cm⁻¹): 3439 (NH); 1738 (cyclic amidic C=O); 1683 (C=O); 1605 (C=N); 1246, 1068 (C-S-C). ¹H-NMR (DMSO-d₆, δ ppm): 3.79 (d, *J* = 11.2 Hz, 2H, thiazolidinone-C₅-H); 3.83 (s, 3H, OCH₃); 7.01 (t, *J* = 7.7 Hz, 1H, thiazolidinone-N-phenyl-C₄-H); 7.06 (d, *J* = 8.4 Hz, 2H, methoxyphenyl-C_{3,5}-H); 7.32-7.43 (m, 3H, phenyl-C₄-H and thiazolidinone-N-phenyl-C_{3,5}-H); 7.55-7.59 (m, 4H, phenyl-C_{3,5}-H and thiazolidinone-N-phenyl -C_{2,6}-H); 7.85 (d, *J* = 8.4 Hz, 2H, methoxyphenyl-C_{3,5}-H); 7.99 (d, *J* = 7.7, 2H, phenyl-C_{2,6}-H); 9.10 (s, 1H, pyrazole-C₅-H); 10.55 (s, 1H, NH). Elemental analysis Calcd for C₂₆H₂₁N₅O₃S: C, 64.58; H, 4.38; N, 14.48; S, 6.63. Found: C, 64.81; H, 4.43; N, 14.63; S, 6.70

5.1.6.2 N'-(3-Allyl-4-oxothiazolidin-2-ylidene)-3-(4-methoxyphenyl)-1-phenyl-1H-pyrazole-4-carbohydrazide 6b

The product was crystallized from DMF: H₂O (9:1) as white solid, mp 148-150 °C, in yield (93%). IR (cm⁻¹): 3130 (NH); 1698, 1653 (C=O); 1607 (C=N); 1068 (C-S-C). ¹H-NMR (DMSO-d₆, δ ppm): 3.77, 3.97 (2s, 2H, thiazolidinone-C₅-H, *E* and *Z* isomers); 3.80 (s, 3H, OCH₃); 3.81, 4.24 (2d, *J* = 5.6 Hz, 2H, CH₂=CH-CH₂, *E* and *Z* isomers); 4.13, 4.37 (2d, *J* = 10.4 Hz, 1H, H_{cis}-CH₂=CH-CH₂, *E* and *Z* isomers); 4.24, 4.75 (2d, *J* = 17.2 Hz, 1H, H_{trans}-CH₂=CH-CH₂-); 5.02-5.08 and 5.64-5.69 (2m, 1H, CH₂=CH-CH₂, *E* and *Z* isomers); 6.98, 7.01 (2d, *J* = 8.7 Hz, 2H, methoxyphenyl-C_{3,5}-H, *E* and *Z* isomers); 7.37-7.39 (m, 2H, phenyl-C₄-H, *E* and *Z* isomers); 7.49-7.58 (m, 4H, phenyl-C_{3,5}-H, *E* and *Z* isomers); 7.78 (d, *J* = 8.7 Hz, 2H, methoxyphenyl-C_{2,6}-H); 7.84-7.89 (m, 4H, phenyl-C_{2,6}-H and methoxyphenyl-C_{2,6}-H); 7.98 (d, *J* = 7.8 Hz, 2H, phenyl-C_{2,6}-H); 8.79, 8.88 (2s, 1H, pyrazole-C₅-H, *E* and *Z* isomers); 9.09, 9.40 (2s, 1H, NH, D₂O-exchangeable, *E* and *Z* isomers). Elemental analysis Calcd for C₂₃H₂₁N₅O₃S: C, 61.73; H, 4.73; N, 15.65; S, 7.17. Found: C, 62.02; H, 4.80; N, 15.89; S, 7.23.

5.2.7. General method for preparation of N'-[3-(Phenyl/allyl)-4-(phenyl/4-bromophenyl)thiazol-2(3H)-ylidene]-3-(4-methoxy phenyl)-1-phenyl-1H-pyrazole-4-carbohydrazides 7a-d

To a suspension of substituted thiosemicarbazide **5a** or **5b** (1 mmol) in absolute ethanol (10 ml), phenacyl bromide or *p*-Br-phenacyl bromide (1 mmol) and anhydrous Na acetate (0.08 g, 1 mmol) were added. The reaction mixture was heated under reflux for (8-10) h, then cooled and the precipitate formed was filtered, washed with H₂O, dried and crystallized from ethanol.

5.1.6.3 *N'*-(3,4-Diphenylthiazol-2(3H)-ylidene)-3-(4-methoxyphenyl)-1-phenyl-1H-pyrazole-4-carbohydrazide **7a**

The product was obtained as white solid, mp 230-232 °C, in yield (82%). IR (cm⁻¹): 3177 (NH); 1677 (C=O); 1582 (C=N); 1248, 1063 (C-S-C). ¹H -NMR (DMSO-d₆, δ ppm): 3.82 (s, 3H, OCH₃); 6.98-7 (m, 2H, thiazole-N-phenyl-C₄-H and thiazole-C₅-H); 7.05 (d, *J* = 8.4 Hz, 2H, methoxyphenyl-C_{3,5}-H); 7.31-7.43 (m, 4H, pyrazole-N-phenyl-C₄-H, phenyl-C₄-H and thiazole-N-phenyl-C_{3,5}-H); 7.54-7.59 (m, 6H, pyrazole-N-phenyl-C_{3,5}-H, thiazole-N-phenyl-C_{2,6}-H and phenyl-C_{3,5}-H); 7.85 (d, *J* = 8.4 Hz, 2H, methoxyphenyl-C_{2,6}-H); 7.99 (d, *J* = 7.8 Hz, 4H, pyrazole-N-phenyl-C_{2,6}-H and phenyl-C_{2,6}-H); 9.08 (s, 1H, pyrazole-C₅-H); 10.52 (s, 1H, NH, D₂O-exchangeable). Elemental analysis Calcd for C₃₂H₂₅N₅O₂S: C, 70.70; H, 4.64; N, 12.88; S, 5.90. Found: C, 70.89; H, 4.68; N, 13.17; S, 5.98.

5.1.6.4 *N'*-[4-(4-Bromophenyl)-3-phenylthiazol-2(3H)-ylidene]-3-(4-methoxyphenyl)-1-phenyl-1H-pyrazole-4-carbohydrazide **7b**

The product was obtained as white solid, mp 233-235 °C, in yield (79%). IR (cm⁻¹): 3179 (NH); 1678 (C=O); 1582 (C=N); 1249, 1063 (C-S-C); 742 (C-Br). ¹H -NMR (400 MHz, DMSO-d₆, δ ppm): 3.82 (s, 3H, OCH₃); 6.99-7.02 (m, 2H, thiazole-N-phenyl-C₄-H and thiazole-C₅-H); 7.06 (d, *J* = 8.4 Hz, 2H, methoxyphenyl-C_{3,5}-H); 7.32-7.42 (m, 4H, bromophenyl-C_{2,6}-H and thiazole-N-C₆H₅-C_{3,5}-H); 7.55-7.59 (m, 5H, methoxyphenyl-C_{2,6}-H and pyrazole-N-phenyl-C_{3,4,5}-H); 7.85 (d, *J* = 8.36 Hz, 2H, bromo phenyl-C_{3,5}-H); 7.99 (d, *J* = 7.8 Hz, 4H, pyrazole-N-phenyl-C_{2,6}-H and thiazole-N-phenyl-C_{2,6}-H); 9.09 (s, 1H, pyrazole-C₅-H); 10.55 (s, 1H, NH, D₂O-exchangeable). ¹³C-NMR (100 MHz, DMSO-d₆, δ ppm): 55.68 (OCH₃); 106.15 (thiazole-C₅); 114.3 (methoxyphenyl-C_{3,5}); 114.28 (pyrazole-C₄); 117.5 (Br-phenyl-C₄); 117.53 (thiazole-N-phenyl-C_{2,6}); 119.36 (phenyl-C_{2,6}); 119.38 (thiazole-N-phenyl-C₄); 122.28 (methoxyphenyl-C₁); 124.43 (phenyl-C₄); 127.67 (pyrazole-C₅); 129.51 (methoxy phenyl-C_{2,6} and Br-Phenyl-C_{2,6}); 130.16 (phenyl-C_{3,5}, thiazole-N-phenyl-C_{3,5}, Br-phenyl-C_{1,3,5}); 130.78 (phenyl-C₁); 139.17 (thiazole-N-phenyl-C₁); 139.31 (thiazole-C₄); 150.58 (thiazole-C₂); 153.42 (pyrazole-C₃); 160.07 (methoxyphenyl-C₄); 160.23 (C=O). EIMS *m/z* (% relative abundance): 623 (5) (M⁺+2), 621 (5) (M⁺), 335 (7), 323 (6), 319 (5), 271 (6), 242 (7), 225 (25), 223 (9), 204 (6), 175 (12), 138 (12), 135 (100), 109 (53), 104 (21), 97 (17), 54 (24). Elemental analysis Calcd for C₃₂H₂₄BrN₅O₂S: C, 61.74; H, 3.89; N, 11.25; S, 5.15. Found: C, 61.89; H, 3.87; N, 11.48; S, 5.23.

5.1.6.5 *N'*-(3-Allyl-4-phenylthiazol-2(3H)-ylidene)-3-(4-methoxyphenyl)-1-phenyl-1H-pyrazole-4-carbohydrazide 7c

The product was obtained as yellowish brown solid, mp 119-121 °C, in yield (75%). IR (cm⁻¹): 3440 (NH); 1673 (C=O); 1598 (C=N); 1248, 1056 (C-S-C). ¹H-NMR (DMSO-d₆, δ ppm): 3.82 (s, 3H, OCH₃); 3.85 (d, *J* = 5.6 Hz, 2H, CH₂=CH-CH₂); 5.13 (d, *J* = 10.4 Hz, 1H, H_{cis}-CH₂=CH-CH₂); 5.24 (d, *J* = 17.2 Hz, 1H, H_{trans}-CH₂=CH-CH₂); 5.85-5.95 (m, 1H, CH₂=CH-CH₂); 7.03 (d, *J* = 8.6 Hz, 2H, methoxy phenyl-C_{3,5}-H); 7.39 (t, *J* = 7.6 Hz, 2H, N-phenyl-C₄-H and phenyl-C₄-H); 7.54-7.72 (m, 5H, N-phenyl-C_{3,5}-H, phenyl-C_{3,5}-H and thiazole-C₅-H); 7.84-7.87 (m, 4H, methoxy phenyl-C_{2,6}-H and phenyl-C_{2,6}-H); 7.98 (d, *J* = 7.6 Hz, 2H, N-phenyl-C_{2,6}-H); 9.03 (s, 1H, pyrazole-C₅-H). ¹³C-NMR (DMSO-d₆, δ ppm): 45.36 (CH₂=CH-CH₂); 55.69 (OCH₃); 106.64 (thiazole-C₅); 114.17 (methoxyphenyl-C_{3,5} and pyrazole-C₄); 116.39 (CH₂=CH-CH₂); 119.28 (N-phenyl-C_{2,6}); 124.54 (methoxyphenyl-C₁); 124.54 (2 phenyl-C₄); 129.08 (phenyl-C₁); 129.91 (pyrazole-C₅); 130.12 (methoxyphenyl-C_{2,6} and phenyl-C_{2,6}); 130.38 (2 phenyl-C_{3,5}); 135.17 (CH₂=CH-CH₂ and thiazole-C₄); 139.34 (N-phenyl-C₁); 150.29 (thiazole-C₂); 153.18 (pyrazole-C₃); 160.14 (methoxyphenyl-C₄); 163.61 (C=O). Elemental analysis Calcd for C₂₉H₂₅N₅O₂S: C, 68.62; H, 4.96; N, 13.80; S, 6.32. Found: C, 68.90; H, 4.99; N, 14.07; S, 6.41.

5.1.6.6 *N'*-[3-Allyl-4-(4-bromophenyl)thiazol-2(3H)-ylidene]-3-(4-methoxyphenyl)-1-phenyl-1H-pyrazole-4-carbohydrazide 7d

The product was obtained as brown solid, mp 128-130 °C, in yield (72%). IR (cm⁻¹): 3194 (NH); 1673 (C=O); 1595 (C=N); 1247, 1062 (C-S-C); 755 (C-Br). ¹H-NMR (DMSO-d₆, δ ppm): 3.82 (s, 3H, OCH₃); 3.85 (d, *J* = 5.6 Hz, 2H, CH₂=CH-CH₂); 5.13 (d, *J* = 10.4 Hz, 1H, H_{cis}-CH₂=CH-CH₂); 5.24 (d, *J* = 17.2 Hz, 1H, H_{trans}-CH₂=CH-CH₂); 5.88-5.95 (m, 1H, CH₂=CH-CH₂); 7.03 (d, *J* = 8.6 Hz, 2H, methoxyphenyl-C_{3,5}-H); 7.39 (t, *J* = 7.6 Hz, 1H, phenyl-C₄-H); 7.54-7.77 (m, 5H, bromophenyl-C_{2,6}-H, phenyl-C_{3,5}-H and thiazole-C₅-H); 7.85 (d, *J* = 8.6 Hz, 4H, methoxyphenyl-C_{2,6}-H and bromo phenyl-C_{3,5}-H); 7.98 (d, *J* = 7.7 Hz, 2H, phenyl-C_{2,6}-H); 9.03 (s, 1H, pyrazole-C₅-H). Elemental analysis Calcd for C₂₉H₂₄BrN₅O₂S: C, 59.39; H, 4.12; N, 11.94; S, 5.47. Found: C, 59.64; H, 4.18; N, 12.17; S, 5.60.

5.2.8. General method for preparation of 3-[3-(4-Methoxyphenyl)-1-phenyl-1H-pyrazol-4-yl]-4-(phenyl/allyl)-1H-1,2,4-triazole-5(4H)-thiones 8a,b

A suspension of substituted thiosemicarbazide **5a** or **5b** (1 mmol) in ethanol (10 ml) was dissolved in aqueous KOH (3 ml, 4N). The reaction mixture was gently heated under reflux for 3 h, then it was concentrated and cooled to room temperature. The pH of the reaction mixture was adjusted to 5-6 with dilute HCl and the solid formed was filtered, washed with H₂O, dried and crystallized from appropriate solvents.

5.1.6.7 3-[3-(4-Methoxyphenyl)-1-phenyl-1H-pyrazol-4-yl]-4-phenyl-1H-1,2,4-triazole-5(4H)-thione 8a

The product was crystallized from DMF:H₂O (9:1) as white solid, mp 253-255 °C, in yield (94%). IR (cm⁻¹): 3421 (NH); 1598 (C=N); 1501, 1247, 1220 and 957 (N-C=S I, II, III and IV bands, respectively). ¹H -NMR (DMSO-d₆, δ ppm): 3.79 (s, 3H, OCH₃); 6.95 (d, *J* = 8.4 Hz, 2H, methoxyphenyl-C_{3,5}-H); 7.07-7.15 (m, 2H, triazole-N-phenyl-C_{2,6}-H); 7.20-7.38 (m, 6H, pyrazole-N-phenyl-C_{3,4,5}-H and triazole-N-phenyl-C_{3,4,5}-H); 7.49-7.54 (m, 2H, pyrazole-N-phenyl-C_{2,6}-H); 7.77 (d, *J* = 8.4 Hz, 2H, methoxyphenyl-C_{2,6}-H); 8.69 (s, 1H, pyrazole-C₅-H); 14.16 (s, 1H, SH, D₂O-exchangeable). Elemental analysis Calcd for C₂₄H₁₉N₅OS: C, 67.74; H, 4.50; N, 16.46; S, 7.54. Found: C, 67.98; H, 4.47; N, 16.72; S, 7.69.

5.1.6.8 4-Allyl-3-[3-(4-methoxyphenyl)-1-phenyl-1H-pyrazol-4-yl]-1H-1,2,4-triazole-5(4H)-thione 8b

The product was crystallized from ethanol as off-white solid, mp 186-188 °C, in yield (95%). IR (cm⁻¹): 3421 (NH); 1608 (C=N); 1503, 1249, 1087 & 957 (N-C=S I, II, III & IV bands, respectively). ¹H -NMR (DMSO-d₆, δ ppm): 3.78 (s, 3H, OCH₃); 4.49 (d, *J* = 5.2 Hz, 2H, CH₂=CH-CH₂); 4.79 (d, *J* = 17.2 Hz, 1H, H_{trans}-CH₂=CH-CH₂); 4.99 (d, *J* = 10.4 Hz, 1H, H_{cis}-CH₂=CH-CH₂); 5.62-5.69 (m, 1H, CH₂=CH-CH₂); 7.01 (d, *J* = 8.6 Hz, 2H, methoxy phenyl-C_{3,5}-H); 7.38 (t, *J* = 7.6 Hz, 1H, phenyl-C₄-H) 7.49 (d, *J* = 7.8 Hz, 2H, phenyl-C_{3,5}-H); 7.55-7.59 (m, 2H, phenyl-C_{2,6}-H) 7.93 (d, *J* = 8.6 Hz, 2H, methoxyphenyl-C_{2,6}-H); 8.9 (s, 1H, pyrazole-C₅-H); 14.02 (s, 1H, SH, D₂O-exchangeable). ¹³C-NMR (DMSO-d₆, δ ppm): 45.88 (CH₂=CH-CH₂); 55.66 (OCH₃); 106.21 (pyrazole-C₄); 114.66 (methoxyphenyl-C_{3,5}); 118.11 (CH₂=CH-CH₂); 119.23 (phenyl-C_{2,6}); 124.38 (methoxyphenyl-C₁); 127.62 (2phenyl-C₄); 128.90 (methoxyphenyl-C_{2,6}); 130.17 (phenyl-C_{3,5}); 131.64 (pyrazole-C₅); 131.72 (CH₂=CH-CH₂); 139.39 (phenyl-C₁); 145.69 (triazole-C₂); 151.06 (pyrazole-C₃); 160.14 (methoxy phenyl-C₄); 167.53 (triazole-C₅). Elemental analysis Calcd for C₂₁H₁₉N₅OS: C, 64.76; H, 4.92; N, 17.98; S, 8.23. Found: C, 64.98; H, 4.96; N, 18.23; S, 8.30.

5.2.9. General method for preparation of 5-[3-(4-Methoxyphenyl)-1-phenyl-1H-pyrazol-4-yl]-N-(phenyl/allyl)-1,3,4-thiadiazol-2-amines 9a,b

The substituted thiosemicarbazide **5a** or **5b** (1 mmol) was added gradually with stirring on an ice-cold conc H₂SO₄ (5 ml) and the reaction mixture was further stirred for 4 h in ice bath. The reaction mixture was poured onto ice-H₂O mixture. The pH of the solution was adjusted to 7-8 with NH₄OH solution and the resulting solid was filtered, washed with H₂O, dried and crystallized from appropriate solvents.

5.1.6.9 2-[3-(4-Methoxyphenyl)-1-phenyl-1H-pyrazol-4-yl]-N-phenyl-1,3,4-thiadiazol-5-amine 9a

The product was crystallized from DMF:H₂O (9:1) as greenish yellow solid, mp 192-194 °C, in yield (95%). IR (cm⁻¹): 3178 (NH); 1612 (C=N); 1202, 1072 (C-S-C). ¹H -NMR (DMSO-d₆, δ ppm): 3.83 (s, 3H, OCH₃); 5.67 (s, 1H, NH, D₂O-exchangeable); 7.09 (d, *J* = 8.5 Hz, 2H, methoxyphenyl-C_{3,5}-H); 7.11-7.24 (m, 1H, NH-phenyl-C₄-H); 7.31-7.39 (m, 3H, NH-phenyl - C_{3,5}-H and phenyl-C₄-H); 7.51-7.70 (m, 6H, phenyl-C_{2,3,5,6}-H and NH-phenyl-C_{2,6}-H); 7.97 (d, *J* = 8.5 Hz, 2H, methoxyphenyl-C_{2,6}-H); 9.06 (s, 1H, pyrazole-C₅-H). ¹³C-NMR (DMSO-d₆, δ ppm): 56.22 (OCH₃); 112.25 (pyrazole-C₄); 112.66 (NH-phenyl-C_{2,6}); 116.90 (methoxy phenyl-C_{3,5}); 119.15 (phenyl-C_{2,6}); 123.17 (NH-phenyl-C₄); 127.01 (methoxyphenyl-C_{2,6}); 127.53 (methoxyphenyl-C₁); 129.37 (phenyl-C₄); 130.14 (phenyl-C_{3,5}); 132.08 (NH-phenyl-C_{3,5}); 134.90 (pyrazole-C₅); 139.30 (NH-phenyl-C₁); 141.16 (phenyl-C₁); 150.38 (pyrazole-C₃); 150.50 (thiadiazole-C₂); 157.17 (methoxy phenyl-C₄); 164.06 (thiadiazole-C₅). Elemental analysis Calcd for C₂₄H₁₉N₅OS: C, 67.74; H, 4.50; N, 16.46; S, 7.54. Found: C, 67.88; H, 4.57; N, 16.80; S, 7.62.

5.1.6.10 N-Allyl-5-[3-(4-methoxyphenyl)-1-phenyl-1H-pyrazol-4-yl]-1,3,4-thiadiazol-2-amine 9b

ethanol as pale yellow solid, mp 140-142 °C, in yield (92%). IR (cm⁻¹): 3201 (NH); 1600 (C=N); 1222 & 1056 (C-S-C). ¹H -NMR (DMSO-d₆, δ ppm): 3.26 (d, *J* = 10.8 Hz, 1H, H_{cis}-CH₂=CH-CH₂-); 3.40 (d, *J* = 16.7 Hz, 1H, H_{trans}-CH₂=CH-CH₂-); 3.82 (s, 3H, OCH₃); 3.87 (d, *J* = 5.9 Hz, 2H, CH₂=CH-CH₂-); 4.59 (m, 1H, CH₂=CH-CH₂-, masked by DMSO); 7.08 (d, *J* = 8.4 Hz, 2H, methoxyphenyl-C_{3,5}-H); 7.39 (t, *J* = 7.6, 1H, phenyl-C₄-H); 7.52-7.56 (m, 2H, phenyl-C_{3,5}-H); 7.67 (d, *J* = 8.4 Hz, 2H, methoxyphenyl-C_{2,6}-H); 7.96 (d, *J* = 7.8 Hz, 2H, phenyl-C_{2,6}-H); 9.15 (s, 1H, pyrazole-C₅-H); 9.46 (s, 1H, NH, D₂O-exchangeable). Elemental analysis Calcd for C₂₁H₁₉N₅OS: C, 64.76; H, 4.92; N, 17.98; S, 8.23. Found: C, 65.01; H, 4.97; N, 18.19; S, 8.31.

5.1.6.11 General method for preparation of 5-[3-(4-Methoxyphenyl)-1-phenyl-1H-pyrazol-4-yl]-N-(phenyl/allyl)-1,3,4-oxadiazol-2-amines 10a,b

A mixture of substituted thiosemicarbazide **5a** or **5b** (1 mmol) and mercuric oxide (2.16 g, 10 mmol) in dioxane (20 ml) was heated under reflux for 10 h, then filtered while hot and the precipitate washed with hot dioxane. The filtrate was concentrated, cooled and the precipitate formed was filtered, dried and crystallized from dioxane: H₂O (9:1).

5.1.6.12 2-[3-(4-Methoxyphenyl)-1-phenyl-1H-pyrazol-4-yl]-N-phenyl-1,3,4-oxadiazol-5-amine 10a

The product was obtained as brownish yellow solid, mp 160-162 °C, in yield (75%). IR (cm⁻¹): 3396 (NH); 1675, 1580 (C=N). ¹H -NMR (DMSO-d₆, δ ppm): 3.82 (s, 3H, OCH₃); 7 (t, *J* =

7.36 Hz, 1H, NH-phenyl-C₄-H); 7.05 (d, $J = 8.8$ Hz, 2H, methoxyphenyl-C_{3,5}-H); 7.34-7.40 (m, 3H, phenyl-C₄-H and NH-phenyl-C_{3,5}-H); 7.53-7.55 (m, 2H, phenyl-C_{3,5}-H); 7.64 (d, $J = 7.6$ Hz, 1H, NH-phenyl-C_{2,6}-H); 7.69 (d, $J = 8.8$ Hz, 2H, methoxyphenyl-C_{2,6}-H); 7.98 (d, $J = 7.8$ Hz, 2H, phenyl-C_{2,6}-H); 9.09 (s, 1H, pyrazole-C₅-H); 10.39 (s, 1H, NH, D₂O-exchangeable). Elemental analysis Calcd for C₂₄H₁₉N₅O₂: C, 70.40; H, 4.68; N, 17.10. Found: C, 70.58; H, 4.76; N, 17.34.

5.1.6.13 *N*-Allyl-2-[3-(4-methoxyphenyl)-1-phenyl-1H-pyrazol-4-yl]-1,3,4-oxadiazol-5-amine 10b

The product was obtained as white solid, mp 138-140 °C, in yield (80%). IR (cm⁻¹): 3420 (NH); 1673, 1599 (C=N). ¹H-NMR (DMSO-d₆, δ ppm): 33.82 (s, 3H, OCH₃); 3.86 (d, $J = 5.6$ Hz, 2H, CH₂=CH-CH₂); 5.13 (d, $J = 10.4$ Hz, 1H, H_{cis}-CH₂=CH-CH₂); 5.24 (d, $J = 17.2$ Hz, 1H, H_{trans}-CH₂=CH-CH₂); 5.88-5.98 (m, 1H, CH₂=CH-CH₂); 7.03 (d, $J = 8.6$ Hz, 2H, methoxy phenyl-C_{3,5}-H); 7.39 (t, $J = 7.4$ Hz, 1H, phenyl-C₄-H); 7.53-7.58 (m, 2H, phenyl-C_{3,5}-H); 7.85 (d, $J = 8.6$ Hz, 2H, methoxyphenyl-C_{3,5}-H); 7.98 (d, $J = 7.7$ Hz, 2H, phenyl-C_{2,6}-H); 9.03 (s, 1H, pyrazole-C₅-H). ¹³C-NMR (DMSO-d₆, δ ppm): 45.36 (CH₂=CH-CH₂); 55.68 (OCH₃); 106.64 (pyrazole-C₄); 114.18 (methoxyphenyl-C_{3,5}); 116.38 (CH₂=CH-CH₂); 119.25 (phenyl-C_{2,6}); 124.54 (methoxyphenyl-C₁); 127.55 (phenyl-C₄); 130.12 (methoxyphenyl-C_{2,6} and phenyl-C_{3,5}); 130.37 (pyrazole-C₅); 135.17 (CH₂=CH-CH₂); 139.34 (phenyl-C₁); 150.28 (pyrazole-C₃); 153.18 (oxadiazole-C₅); 160.15 (methoxy phenyl-C₄); 163.61 (oxadiazole-C₂). Elemental analysis Calcd for C₂₁H₁₉N₅O₂: C, 67.55; H, 5.13; N, 18.76. Found: C, 67.79; H, 5.19; N, 18.97.

5.2 *In silico* experiments

5.2.1 Molecular docking

The coordinates for wildtype (PDB code:1j3i) and quadruple mutant (N51I, C59R, S108N and I164L) *pf* DHFR-TS (PDB code:1j3k) crystal structures were retrieved from the protein data bank and handled consequently with MOE [59]. Redundant chains, non-essential ions, water molecules and ligands were discarded. Only exception was made for one structural water molecule that mediates salt-bridge for the co-crystal ligand for both crystal structures. The preparation procedure was conducted by the “Quick Prep” module at default settings. The PDB files were converted to PDBQT files by employing a python script (*prepare_receptor4.py*) provided by the MGLTools package (version 1.5.4) [60] for AutoDock Vina (version 1.1.2) [61] docking experiments.

The most active compounds (**4b**, **4c**, **7a** and **7d**) were built and prepared by MOE. ‘Molecule wash’ function was used to generate meaningful protonation states by deprotonating strong acids and protonating strong bases (if required). Energy minimization of all molecules was performed using the Amber: 10EHT force field at a gradient of 0.01 RMSD. Conformational

search was conducted to sample maximum number of minimized conformations including different stereoisomers and ring conformations (if necessary) using “Stochastic” method, with option “Allow unconstrained double bond rotation” enabled to sample different geometrical isomers of the double bond-containing compounds. All other options were set at default levels. The resulting conformers were saved as SD file for the docking experiments. The SD files were converted and split into PDB files by MOE, which were further converted into PDBQT files by a MGLTools (version 1.5.4) python script (*prepare_ligand4.py*) for AutoDock Vina docking experiments.

AutoDock Vina (version 1.1.2) was used for docking experiments of the most active compounds against both wildtype and quadruple mutant (N51I, C59R, S108N and I164L) *pf* DHFR-TS structures. We employed default docking parameters and the size of the docking grid was 20 Å × 20 Å × 20 Å, with a grid spacing of 1 Å. By default, the docking was terminated when the maximum energy difference between the best scored pose and the worst one was 3 kcal/ mol. Figures 3-5 were rendered using Pymol v2.2 [62]. This docking setup was validated by successful pose-retrieval docking experiment for the co-crystal ligand on both PDB crystal structures.

5.2.2 *In silico* prediction of physicochemical properties, pharmacokinetic profiles, drug likeness scores and toxicity profiles

In the present work, the biologically active compounds were subjected to prediction of the physical and molecular properties using various tools, such as PreADMET, Molinspiration, Mol-Soft and Osiris softwares. Molinspiration chemoinformatic server was used to calculate Lipinski's violation, topological polar surface area (PSA) and percentage of oral absorption (%ABS) [63]. While, PreADMET calculator was used to predict the pharmacokinetic properties, such as absorption, distribution, metabolism, excretion and toxicity [64]. Drug likeness score and solubility parameters were calculated using Mol-Soft software [65], while toxicity risks like mutagenicity, tumorigenicity, irritation and reproductive side effects were calculated using Osiris property explorer [66].

5.3 Biological Screening

5.3.1 *In vivo* antimalarial activity testing against *P. berghei*

A 4-day suppressive test using *P. berghei* ANKA strain infected mice was used for *in vivo* antimalarial screening of the newly synthesized compounds as described by Fidock *et al* [54]. It is the most widely used preliminary test as the efficacy of a compound is calculated in the form of percentage suppression in blood parasitemia level. So efficacy is assessed by a comparison of blood parasitemia levels in treated and untreated mice [67]. On day 0, the test mice were injected intravenously with 0.2 ml of 2×10^7 parasitized

erythrocytes infected with *P. berghei* ANKA strain. These parasitized erythrocytes were obtained from the blood of a donor mouse with approximately 20-30 % parasite and the blood was diluted with normal saline. After 2 h injection, the infected mice were weighed and randomly divided into 47 groups of five mice per cage. Treatment groups were the groups from 1-45 (45 cages) and they received the synthesized compounds orally, each at a dose of 0.048 mmol/kg/day [67]. The negative control group (group 46) received the vehicle, which consisted of 7% Tween and 3% ethanol in distilled water. The positive control group (group 47) received the reference drug, chloroquine phosphate, at a dose of 0.048 mmol/kg/day (25 mg/kg/day). On days 1-3, every 24 h interval, the treatment groups received the same single dose of the synthesized compounds orally as in day 0. On day 4, after 96 h post infection, blood smears from all test animals was prepared using Giemsa stain and level of parasitemia was determined microscopically by counting 5 fields of approximately 100 erythrocytes per field. The difference between the mean value for the negative control group (taken as 100%) and those of the experimental groups was calculated and expressed as percent suppression or activity. The survival time for each test mouse was recorded and the mean survival time was calculated in comparison with that of the negative group. On the other hand, the survival time for chloroquine treated mice was not recorded since they were completely cured from the parasite [68]. Percentage parasitemia and percentage suppression were calculated using the following equations:

$$\% \text{ parasitemia} = \frac{\text{Number of infected RBC}}{\text{Number of total RBC}} \times 100$$

$$\% \text{ Suppression} = \frac{\text{Parasitemia in negative control} - \text{parasitemia in treatment group}}{\text{Parasitemia in negative control}} \times 100$$

5.3.2 *In vitro* antimalarial activity testing against *P. falciparum*

In vitro antimalarial activity was evaluated for the most active compounds which showed reasonable activity in *in vivo* screening. We evaluated their antiplasmodial activity against chloroquine resistant *P. falciparum* strain (RKL9) which was maintained in a continuous culture using the standard method described by Trager and Jensen [55]. The assay was carried out in 96-well microtitre flat-bottomed tissue culture plates incubated at 37°C for 24 h in the presence of two-fold serial dilutions of test compounds and chloroquine diphosphate, which were examined for their effect on schizont maturation. The initial culture

was maintained in small vials with 10% haematocrit, i.e. 10 ml erythrocytes containing 1.0% ring stage parasite in 100 ml complete media and the assay culture volume was 100 ml per well. Number of parasites for the assay was adjusted to 1-1.5% by dilution with fresh human B (+) RBC. Compounds to be evaluated were dissolved in ethanol and further diluted with RPMI 1640 medium while chloroquine diphosphate was dissolved in aqueous medium. Test was done in duplicate wells for each dose of the drugs. Solvent control culture containing the same concentrations of the solvent as present in the test wells was done with RPMI-1640 containing 10% AB (+) serum. Growth of the parasite from solvent control culture was unaffected, while that from duplicate wells of each concentration was affected. Giemsa stained blood smears were used to monitor the affected growth in duplicate wells by counting number of schizont per 100 asexual parasites. Furthermore, percent schizont maturation inhibition was calculated using the equation:

$$1 - N_t/N_c \times 100$$

Where, N_t and N_c are the numbers of schizonts in the test and control wells, respectively.

5.3.3 Toxicity studies

5.3.3.1 Red blood cell hemolysis assay

Red blood cell hemolytic activity and anti-inflammatory activity were assessed generally according to Chatterjee *et al* [56] and Evans *et al* [57]. The experimental steps were performed as reported earlier [32].

5.3.3.2 White blood cell cytotoxicity assessment

In order to determine the safe concentrations of tested compounds that could be used for *in vitro* cell culture; normal peripheral blood mononuclear cells (PBMC) were isolated from a healthy individual by Ficoll-Hypaque (density 1.077 g/L, Lonza, USA) gradient centrifugation. PBMC were collected and washed using HBSS, and then cell viability and count was determined using Trypan blue exclusion test. The experimental steps were performed as reported earlier [32].

5.3.3.3 In vivo acute toxicity testing

Evaluation of acute oral toxicity of the most active antimalarial compounds **4b**, **4c**, **7a** and **7d** was done. For the experimental test, 21 groups of mice, each group containing six male mice weighing 25-30 g each were used [69]. The mice were fasted overnight and weighed before the test and the test compounds were prepared in suspension form in aqueous vehicle containing 1% gum acacia. Five groups of mice were used for each compound receiving the test compounds following the experimental steps as reported earlier [32].

6 Acknowledgement

Authors would like to express their sincere thanks towards Alexandria University-Research Enhancement Program (ALEXREP), for their financial and logistical support through the Research Project (HLTH-13, BASIC-13). Also, TMI would like to thank Prof. Frank Boeckler (Lab. of Molecular Design and Pharmaceutical Biophysics, Eberhard Karls University of Tuebingen) for granting access to some computational tools.

7 Ethical conduct of research

The protocols used in this study followed the guidelines set in 'The Guide for the Care and Use of Laboratory Animals', and obtained approval By Animal Care & Use Committee (ACUC), Faculty of Pharmacy, Alexandria University, No. ACUC17/18 at 29/4/2017.

8 References

- [1] T. Spangenberg, J.N. Burrows, P. Kowalczyk, S. McDonald, T.N. Wells, P. Willis, The open access malaria box: a drug discovery catalyst for neglected diseases, *PloS one*, 8 (2013) 62901-62908.
- [2] World Malaria Report 2016. Geneva: World Health Organization; 2016. Licence: CC BY-NC-SA 3.0 IGO.
- [3] E. Molla, B. Ayele, Prevalence of Malaria and Associated Factors in Dilla Town and the Surrounding Rural Areas, Gedeo Zone, Southern Ethiopia, *J. Bacteriol. Parasitol.*, 6 (2015) 1000241-1000247.
- [4] K. Na-Bangchang, J. Karbwang, Current status of malaria chemotherapy and the role of pharmacology in antimalarial drug research and development, *Fundam. Clin. Pharmacol.*, 23 (2009) 387-409.
- [5] J. N Burrows, K. Chibale, T. NC Wells, The state of the art in anti-malarial drug discovery and development, *Curr. Top. Med. Chem.*, 11 (2011) 1226-1254.
- [6] E.L. Flannery, A.K. Chatterjee, E.A. Winzeler, Antimalarial drug discovery [mdash] approaches and progress towards new medicines, *Nat. Rev. Microbiol.*, 11 (2013) 849-862.
- [7] B. Ogutu, Artemether and lumefantrine for the treatment of uncomplicated Plasmodium falciparum malaria in sub-Saharan Africa, *Expert Opin. Pharmacother.*, 14 (2013) 643-654.
- [8] S. Nwaka, A. Hudson, Innovative lead discovery strategies for tropical diseases, *Nat. Rev. Drug Discov.*, 5 (2006) 941-955.
- [9] I.B. Müller, J.E. Hyde, Folate metabolism in human malaria parasites—75 years on, *Mol. Biochem. Parasitol.*, 188 (2013) 63-77.
- [10] W. Pornthanakasem, P. Riengrunroj, P. Chitnumsub, W. Ittarat, D. Kongkasuriyachai, C. Uthaiipibull, Y. Yuthavong, U. Leartsakulpanich, Evaluation for the role of Plasmodium vivax dihydropteroate synthase polymorphisms in sulfa drug resistance, *Antimicrob. Agents Chemother.*, (2016) 01831-01838.
- [11] H.R. Bhat, U.P. Singh, P. Gahtori, S.K. Ghosh, K. Gogoi, A. Prakash, R.K. Singh, Synthesis, Docking, In Vitro and In Vivo Antimalarial Activity of Hybrid 4-aminoquinoline–1, 3, 5-triazine Derivatives Against Wild and Mutant Malaria Parasites, *Chem. Biol. Drug. Des.*, 86 (2015) 265-271.
- [12] M. Kumar, A. Dagar, V.K. Gupta, A. Sharma, In silico docking studies of bioactive natural plant products as putative DHFR antagonists, *Med. Chem. Res.*, 23 (2014) 810-817.

- [13] W. Mokmak, S. Chunsriviro, S. Hannongbua, Y. Yuthavong, S. Tongshima, S. Kamchonwongpaisan, Molecular Dynamics of Interactions between Rigid and Flexible Antifolates and Dihydrofolate Reductase from Pyrimethamine-Sensitive and Pyrimethamine-Resistant Plasmodium falciparum, *Chem. Biol. Drug. Des.*, 84 (2014) 450-461.
- [14] N. Nayak, J. Ramprasad, U. Dalimba, New INH-pyrazole analogs: Design, synthesis and evaluation of antitubercular and antibacterial activity, *Bioorg. Med. Chem. Lett.*, 25 (2015) 5540-5545.
- [15] Y.-R. Li, C. Li, J.-C. Liu, M. Guo, T.-Y. Zhang, L.-P. Sun, C.-J. Zheng, H.-R. Piao, Synthesis and biological evaluation of 1,3-diaryl pyrazole derivatives as potential antibacterial and anti-inflammatory agents, *Bioorg. Med. Chem. Lett.*, 25 (2015) 5052-5057.
- [16] F.J. Meng, T. Sun, W.Z. Dong, M.H. Li, Z.Z. Tuo, Discovery of Novel Pyrazole Derivatives as Potent Neuraminidase Inhibitors against Influenza H1N1 Virus, *Archiv der Pharmazie*, 349 (2016) 168-174.
- [17] H. Chuang, L.-C.S. Huang, M. Kapoor, Y.-J. Liao, C.-L. Yang, C.-C. Chang, C.-Y. Wu, J.R. Hwu, T.-J. Huang, M.-H. Hsu, Design and synthesis of pyridine-pyrazole-sulfonate derivatives as potential anti-HBV agents, *MedChemComm*, 7 (2016) 832-836.
- [18] H.N. Hafez, A.-R.B.A. El-Gazzar, S.A. Al-Hussain, Novel pyrazole derivatives with oxa/thiadiazolyl, pyrazolyl moieties and pyrazolo[4,3-d]-pyrimidine derivatives as potential antimicrobial and anticancer agents, *Bioorg. Med. Chem. Lett.*, 26 (2016) 2428-2433.
- [19] J.B. Shi, W.J. Tang, X.B. qi, R. Li, X.H. Liu, Novel pyrazole-5-carboxamide and pyrazole-pyrimidine derivatives: Synthesis and anticancer activity, *Eur. J. Med. Chem.*, 90 (2015) 889-896.
- [20] A. Özdemir, M.D. Altıntop, Z.A. Kaplancıklı, Ö.D. Can, Ü. Demir Özkay, G. Turan-Zitouni, Synthesis and Evaluation of New 1, 5-Diaryl-3-[4-(methyl-sulfonyl) phenyl]-4, 5-dihydro-1H-pyrazole Derivatives as Potential Antidepressant Agents, *Molecules*, 20 (2015) 2668-2684.
- [21] S. Viveka, P. Shama, S. Naveen, N.K. Lokanath, G.K. Nagaraja, Design, synthesis, anticonvulsant and analgesic studies of new pyrazole analogues: a Knoevenagel reaction approach, *RSC Advances*, 5 (2015) 94786-94795.
- [22] Y.N. Mabkhot, N.A. Kaal, S. Alterary, S.S. Al-Showiman, A. Barakat, H.A. Ghabbour, W. Frey, Synthesis, in-vitro antibacterial, antifungal, and molecular modeling of potent anti-microbial agents with a combined pyrazole and thiophene pharmacophore, *Molecules*, 20 (2015) 8712-8729.
- [23] H.M. Faidallah, M.M. Al-Mohammadi, K.A. Alamry, K.A. Khan, Synthesis and biological evaluation of fluoropyrazolesulfonyleurea and thiourea derivatives as possible antidiabetic agents, *J Enzyme Inhib. Med. Chem.*, (2016) 1-7.
- [24] A.A. Bekhit, A.M. Hassan, H.A.A. El Razik, M.M. El-Miligy, E.J. El-Agroudy, A.E.-D.A. Bekhit, New heterocyclic hybrids of pyrazole and its bioisosteres: Design, synthesis and biological evaluation as dual acting antimalarial-antileishmanial agents, *Eur. J. Med. Chem.*, 94 (2015) 30-44.
- [25] P. Rathelot, N. Azas, H. El-Kashef, F. Delmas, C. Di Giorgio, P. Timon-David, J. Maldonado, P. Vanelle, 1, 3-Diphenylpyrazoles: synthesis and antiparasitic activities of azomethine derivatives, *Eur. J. Med. Chem.*, 37 (2002) 671-679.
- [26] S.C. Karad, V.B. Purohit, J.R. Avalani, N.H. Sapariya, D.K. Raval, Design, synthesis, and characterization of a fluoro substituted novel pyrazole nucleus clubbed with 1, 3, 4-oxadiazole scaffolds and their biological applications, *RSC Advances*, 6 (2016) 41532-41541.
- [27] P. Puthiyapurayil, B. Poojary, C. Chikkanna, S.K. Buridipad, Design, synthesis and biological evaluation of a novel series of 1,3,4-oxadiazole bearing N-methyl-4-(trifluoromethyl) phenyl pyrazole moiety as cytotoxic agents, *Eur. J. Med. Chem.*, 53 (2012) 203-210.
- [28] F.H. Havaladar, A.R. Patil, Syntheses of 1,2,4 triazole derivatives and their biological activity, *E- J. Chem.*, 5 (2008) 347-354.

- [29] P. Majumdar, A. Pati, M. Patra, R.K. Behera, A.K. Behera, Acid Hydrazides, Potent Reagents for Synthesis of Oxygen-, Nitrogen-, and/or Sulfur-Containing Heterocyclic Rings, *Chem. Rev.*, 114 (2014) 2942-2977.
- [30] T.M. Ibrahim, M.R. Bauer, A. Dorr, E. Veyisoglu, F.M. Boeckler, pROC-Chemotype Plots Enhance the Interpretability of Benchmarking Results in Structure-Based Virtual Screening, *J. Chem. Inf. Model.*, 55 (2015) 2297-2307.
- [31] V.A. Chornous, M.K. Bratenko, M.V. Vovk, I.I. Sidorchuk, Synthesis and antimicrobial activity of pyrazole-4-carboxylic acid hydrazides and N-(4-pyrazoyl) hydrazones of aromatic and heteroaromatic aldehydes, *Pharm. Chem. J.*, 35 (2001) 203-205.
- [32] A.A. Bekhit, M.N. Saudi, A.M. Hassan, S.M. Fahmy, T.M. Ibrahim, D. Ghareeb, A.M. El-Seidy, S.M. Al-Qallaf, H.J. Habib, A.B. AE, Synthesis, molecular modeling and biological screening of some pyrazole derivatives as antileishmanial agents, *Future Med. Chem.*, (2018).
- [33] A.E.-W.A.O. Sarhan, On the synthesis and reactions of indole-2-carboxylic acid hydrazide, *Monatsh. Chem. Chem. Mon.*, 132 (2001) 753-763.
- [34] M. Cacic, M. Trkovnik, F. Cacic, E. Has-Schon, Synthesis and Antimicrobial Activity of Some Derivatives on the Basis (7-hydroxy-2-oxo-2H-chromen-4-yl)-acetic Acid Hydrazide, *Molecules*, 11 (2006) 134-147.
- [35] A.-R. Farghaly, H. El-Kashef, Synthesis of some new azoles with antiviral potential, *Arkivoc*, 11 (2006) 76-90.
- [36] M. Kalhor, M. Shabani, I. Nikokar, S.R. Banisaeed, Synthesis, characterization and antibacterial activity of some novel thiosemicarbazides, 1,2,4-Triazol-3-thiols and their S-substituted derivatives, *Iran. J. Pharm. Res.*, 14 (2015) 67-75.
- [37] A. Benmohammed, O. Koumeri, A. Djafri, T. Terme, P. Vanelle, Synthesis of Novel Highly Functionalized 4-Thiazolidinone Derivatives from 4-Phenyl-3-thiosemicarbazones, *Molecules*, 19 (2014) 3068-3083.
- [38] V.A. Mamedov, I.A. Nuretdinov, F.G. Sibgatullina, Synthesis of novel thiazoles bearing hydrazine, thiosemicarbazide, thiazole, and thiazolidinone moieties, *Bull. Acad. Sci. USSR, Div. Chem. Sci.*, 40 (1991) 2470-2474.
- [39] S. Bondock, A.E.-G. Tarhoni, A.A. Fadda, Heterocyclic synthesis with 4-benzoyl-1-cyanoacetylthiosemicarbazide: selective synthesis of some thiazole, triazole, thiadiazine, pyrrolthiazole, and pyrazolo[1,5-a]triazine derivatives, *Monatsh. Chem. Chem. Mon.*, 139 (2008) 153-159.
- [40] S.M.I. Badr, Synthesis and antiinflammatory activity of novel 2,5-disubstituted thiophene derivatives, *Turkish J. Chem.*, 35 (2011) 131-143.
- [41] A.M. Farag, A.S. Mayhoub, T.M.A. Eldebss, A.-G.E. Amr, K.A.K. Ali, N.A. Abdel-Hafez, M.M. Abdulla, Synthesis and Structure-Activity Relationship Studies of Pyrazole-based Heterocycles as Antitumor Agents, *Archiv der Pharmazie*, 343 (2010) 384-396.
- [42] M.R. Mahmoud, W.S.I. Abou-Elmagd, S.S. Abdelwahab, E.-S.A. Soliman, Synthesis and spectral characterisation of novel 2,3-disubstituted quinazolin-4(3H)-one derivatives, *J. Chem. Res.*, 36 (2012) 66-71.
- [43] H.A. Saad, N.A. Osman, A.H. Moustafa, Synthesis and analgesic activity of some new pyrazoles and triazoles bearing a 6,8-dibromo-2-methylquinazoline moiety, *Molecules*, 16 (2011) 10187-10201.
- [44] F. El-Essawy, S. Rady, Synthesis of some N-alkylated 1,2,4-triazoles, 1,3,4-oxadiazoles, and 1,3,4-thiadiazoles based on N-(furan-2-yl-methylidene)-4,6-dimethyl-1H-pyrazolo-[3,4-b]pyridine-3-amine, *Chem. Heterocycl. Compd.*, 47 (2011) 497-506.

- [45] H.A. Abdel-Aziz, N.A. Hamdy, A.M. Farag, I.M.I. Fakhr, Synthesis and Reactions of 3-Methylthiazolo[3,2-a]Benzimidazole-2-Carboxylic Acid Hydrazide: Synthesis of Some New Pyrazole, 1,3-Thiazoline, 1,2,4-Triazole and 1,2,4-Triazolo[3,4-b]-1,3,4-Thiadiazine Derivatives Pendant to Thiazolo[3,2-a]Benzimidazole Moiety, *J. Chin. Chem. Soc.*, 54 (2007) 1573-1582.
- [46] National Center for Biotechnology Information. PubChem Database; Patent=US6610707, <https://pubchem.ncbi.nlm.nih.gov/patent/US6610707> (accessed Sept. 24, 2018). in.
- [47] N. Solak, S. Rollas, Synthesis and antituberculosis activity of 2-(aryl/alkylamino)-5-(4-aminophenyl)-1,3,4-thiadiazoles and their Schiff bases, *Arkivoc*, 12 (2006) 173-181.
- [48] S.M. Gomha, S.M. Riyadh, Synthesis under microwave irradiation of [1,2,4]triazolo[3,4-b][1,3,4]thiadiazoles and other diazoles bearing indole moieties and their antimicrobial evaluation, *Molecules*, 16 (2011) 8244-8256.
- [49] M.T. Abdel-Aal, W.A. El-Sayed, A.H. Abdel Aleem, E.S.H. El Ashry, Synthesis of some functionalized arylaminomethyl-1,2,4-triazoles, 1,3,4-oxa-and thiadiazoles, *Pharmazie*, 58 (2003) 788-792.
- [50] J. Yuvaniyama, P. Chitnumsub, S. Kamchonwongpaisan, J. Vanichtanankul, W. Sirawaraporn, P. Taylor, M.D. Walkinshaw, Y. Yuthavong, Insights into antifolate resistance from malarial DHFR-TS structures, *Nat. Struct. Mol. Biol.*, 10 (2003) 357-365.
- [51] D. Kumar, S.I. Khan, B.L. Tekwani, P. Ponnann, D.S. Rawat, 4-Aminoquinoline-pyrimidine hybrids: synthesis, antimalarial activity, heme binding and docking studies, *Eur. J. Med. Chem.*, 89 (2015) 490-502.
- [52] S.S. Maurya, S.I. Khan, A. Bahuguna, D. Kumar, D.S. Rawat, Synthesis, antimalarial activity, heme binding and docking studies of N-substituted 4-aminoquinoline-pyrimidine molecular hybrids, *Eur. J. Med. Chem.*, 129 (2017) 175-185.
- [53] J. Yuvaniyama, P. Chitnumsub, S. Kamchonwongpaisan, J. Vanichtanankul, W. Sirawaraporn, P. Taylor, M.D. Walkinshaw, Y. Yuthavong, Insights into antifolate resistance from malarial DHFR-TS structures, *Nat. Struct. Mol. Biol.*, 10 (2003) 357-365.
- [54] D.A. Fidock, P.J. Rosenthal, S.L. Croft, R. Brun, S. Nwaka, Antimalarial drug discovery: efficacy models for compound screening, *Nat. Rev. Drug Discov.*, 3 (2004) 509-520.
- [55] W. Trager, J.B. Jensen, Human malaria parasites in continuous culture, *Science*, 193 (1976) 673-675.
- [56] S. Chatterjee, S.N. Das, Anti-arthritis and anti-inflammatory effect of a poly-herbal drug (EASE): Its mechanism of action, *Indian J. Pharmacol.*, 28 (1996) 116-119.
- [57] B.C. Evans, C.E. Nelson, S.Y. Shann, K.R. Beavers, A.J. Kim, H. Li, H.M. Nelson, T.D. Giorgio, C.L. Duvall, Ex vivo red blood cell hemolysis assay for the evaluation of pH-responsive endosomolytic agents for cytosolic delivery of biomacromolecular drugs, *JoVE*, 73 (2013) e50166 50161-50165.
- [58] G. Repetto, A. Del Peso, J.L. Zurita, Neutral red uptake assay for the estimation of cell viability/cytotoxicity, *Nat. Protoc.*, 3 (2008) 1125-1131.
- [59] Molecular Operating Environment (MOE 2016), Chemical Computing Group Inc.: Montreal, <http://www.chemcomp.com>.
- [60] M.F. Sanner, Python: a programming language for software integration and development, *J Mol Graph Model*, 17 (1999) 57-61.
- [61] O. Trott, A.J. Olson, AutoDock Vina: improving the speed and accuracy of docking with a new scoring function, efficient optimization, and multithreading, *J. Comput. Chem.*, 31 (2010) 455-461.
- [62] The PyMOL Molecular Graphics System, Version 2.2 Schrödinger, LLC.
- [63] <http://www.molinspiration.com/>.
- [64] <http://preadmet.bmdrc.org/>.

[65] <http://molsoft.com/mprop/>.

[66] <http://www.organic-chemistry.org/prog/peo/>.

[67] B.S. Kalra, S. Chawla, P. Gupta, N. Valecha, Screening of antimalarial drugs: An overview, *Indian J. Pharmacol.*, 38 (2006) 5-12.

[68] J.N. Dominguez, C. Leon, J. Rodrigues, N.G. de Dominguez, J. Gut, P.J. Rosenthal, Synthesis of chlorovinyl sulfones as structural analogs of chalcones and their antiplasmodial activities, *Eur. J. Med. Chem.*, 44 (2009) 1457-1462.

[69] A.A. Bekhit, A.M. Baraka, Novel milrinone analogs of pyridine-3-carbonitrile derivatives as promising cardiotonic agents, *Eur. J. Med. Chem.*, 40 (2005) 1405-1413.

Highlights:

- ✓ 1,3,4-trisubstituted pyrazole derivatives were synthesized.
- ✓ Promising antimalarial activity against *P. berghei* and chloroquine resistant RKL9.
- ✓ Antimalarial activity is up to 13-fold higher than standard chloroquine phosphate.
- ✓ Molecular docking experiments rationalized the observed antimalarial activity
- ✓ All compounds were well-tolerated up to 150 mg/kg via oral route.
- ✓ RBC hemolysis assay and cytotoxicity assessment showed low toxicity profile.